

# A NUMBER PROJECTED MODEL WITH GENERALIZED PAIRING INTERACTION

**W. Satuła**<sup>1-4</sup> and **R. Wyss**<sup>2,5</sup>

<sup>1</sup> *Institute of Theoretical Physics, Warsaw University, ul. Hoża 69, PL-00 681, Warsaw, Poland*

<sup>2</sup> *Royal Institute of Technology, Physics Department Frescati, Frescativägen 24, S-104 05 Stockholm, Sweden*

<sup>3</sup> *Joint Institute for Heavy Ion Research, Oak Ridge National Laboratory*

*P.O. Box 2008, Oak Ridge, TN 37831, U.S.A.*

<sup>4</sup> *Department of Physics, University of Tennessee, Knoxville, TN 37996, U.S.A.*

<sup>5</sup> *Department of Technology, Kalmar University,*

*Box 905, 391 29 Kalmar, Sweden*

(November 5, 2018)

A mean-field model with a generalized pairing interaction that accounts for neutron-proton pairing is presented. Both the BCS as well as number-projected solutions of the model are presented. For the latter case the Lipkin-Nogami projection technique was extended to encompass the case of non-separable proton-neutron systems. The influence of the projection on various pairing phases is discussed. In particular, it is shown that number-projection allows for mixing of different pairing phases but, simultaneously, acts destructively on the proton-neutron correlations. The basic implications of proton-neutron pairing correlations on nuclear masses are discussed. It is shown that these correlations may provide a natural microscopic explanation of the Wigner energy lacking in mean-field models. A possible phase transition from isovector to isoscalar pairing condensate at high angular momenta is also discussed. In particular predictions for the dynamical moments of inertia for the superdeformed band in <sup>88</sup>Ru are given.

PACS numbers : 21.10.Re, 21.60.Jz, 21.60.Ev, 27.80+w

## I. INTRODUCTION

The strongest effects associated with neutron-proton ( $np$ ) pairing are expected in  $N \approx Z$  nuclei where valence protons and neutrons occupy the same shell-model orbits. The basic properties of the  $np$ -interaction are known from the studies of simple configurations of near closed shell nuclei [1,2]. The isovector ( $T=1$ ) interaction is dominated by the  $J=0^+$  channel but the isoscalar ( $T=0$ )  $np$ -interaction is almost equally attractive in the  $J=1^+$  and stretched  $J=(2j)^+$  channels. The  $T=0$  interaction is on the average stronger than the  $T=1$  force. It may, therefore, lead to the appearance of a static  $T=0$   $np$ -pairing condensate, particularly in heavier  $N \approx Z$  nuclei where the large valence space allows for the creation of many  $np$ -pairs. However, it is not obvious whether these correlations are coherent enough to create this new type of collective mode nor what are the main building blocks or specific experimental fingerprints of such a condensate.

Theoretically,  $np$ -pairing is a challenging subject. It offers new opportunities to probe specific parts of the effective nucleon-nucleon interaction. The generalization of BCS (or HFB) techniques to incorporate and allow for unconstrained interplay of  $T=0$  and  $T=1$  pairs on equal footing is by itself non-trivial. Though the first steps to generalize the BCS theory as well as the first applications were done already in the sixties [3,4,5,6,7,8,9,10,11] (for review of the early efforts see [12]) only recently the first symmetry unconstrained, self-consistent mean-field calculations have been performed [13]. Extensions beyond mean-field, restoring either rigorously or approximately number symmetry and/or isospin symmetry are scarce.

The renaissance in the interest for  $np$ -pairing can be traced back to the fast progress in detection techniques and radioactive ion beam (RIB) programs. First experiments with RIB's are soon to come and are targeted on heavy proton-rich nuclei in particular on  $N \approx Z$  nuclei. They are expected to provide important clues resolving the above mentioned, long standing difficulties in understanding  $np$ -pairing. The observables to look for are obviously those which are expected to be strongly modified by a static  $np$ -pair condensate like deuteron-transfer probability [14,15],  $\beta$  and Gamow-Teller decay rates [16,17] or ground-state and high-spin properties [18,19,20,21,22].

So far no clear, systematic experimental signature of the  $np$ -pairing condensate is known. There are, however, some indirect indications, for example, in recent spectroscopic data in  ${}^{72}_{36}\text{Kr}_{36}$  [23] and  ${}^{74}_{37}\text{Rb}_{37}$  [24]. In the ground state of  ${}^{74}_{37}\text{Rb}_{37}$ , with  $\mathbf{T}=1, \mathbf{T}_z=0$ , the  $\gamma$ -ray energies of the collective  $4^+ \rightarrow 2^+ \rightarrow 0^+$  transitions appear to be similar (isobaric analogues) to  ${}^{74}_{36}\text{Kr}_{38}$ , the  $\mathbf{T}=1, \mathbf{T}_z=1$  nucleus in spite of the expected increase in the dynamical moment of inertia due to blocking of the like-particle superfluidity.<sup>1</sup> This phenomenon has been interpreted as a manifestation of  $T=1$   $np$ -pairing collectivity [24]. At higher spins a transition from  $T=1$  to  $T=0$  band has also been observed. Calculations seem to confirm the  $T=1$   $np$ -collectivity at low-spins and predict an increasing role of the aligned  $T=0$  pairs at higher spins, see Refs. [25,26,27]. In  ${}^{72}_{36}\text{Kr}_{36}$  a rather unexpected delay of the first crossing frequency has been measured [23]. It again may have possible links to  $np$ -pairing, see discussion in [25,27,26,28], although more conventional explanations involving shape vibrations cannot be ruled out.

The strongest evidence for the enhancement of  $np$ -pairing effects seems to come from binding energies. The well known slope discontinuity of the isobaric mass parabola at  $N \approx Z$ , see review [29] and refs. therein, indicates an additional binding energy (Wigner energy) in  $N \approx Z$  nuclei. The Wigner energy is predominantly due to the  $T=0$  interaction [30,31]. However, the mechanism responsible for the extra binding energy seems to be rather complex when expressed in terms of  $np$ -pairs of given  $J, T$  [31]. It cannot be solely explained in terms of  $J=1, T=0$   $np$ -pairs, at least not for  $sd$  or  $pf$  shell nuclei. A connection of the Wigner energy and the  $T=0$   $np$ -pairing condensate was suggested in our Letter [20] based on deformed mean-field calculations with a schematic pairing interaction. Mass measurements of more heavy  $N \approx Z$  nuclei are needed to shed more light on this issue.

The aim of this paper is to further investigate basic features of  $np$ -pairing. The paper supplements the above mentioned letter [20] explaining in more detail certain technical aspects of our model but also provides new numerical and analytical results. The paper is organized as follows: In Sect. II we introduce the basic concepts concerning the Bogolyubov transformation and the self-consistent symmetries (SCS) used here to simplify the calculations. Details concerning the model hamiltonian and implications of SCS on the structure and interpretation of the model can be found in Section III. Section IV presents the method used to restore approximately the particle-number symmetry which is an extension of the so called Lipkin-Nogami technique for the case of a non-separable proton-neutron system. The ideas presented in this section are independent on the kind of two-body interaction used in the calculations. The results of numerical calculations, discussion and conclusions are given in Sections V and VI, respectively.

---

<sup>1</sup>Throughout the paper, the bold-faced symbols  $\mathbf{T}$  and  $\mathbf{T}_z=(N-Z)/2$  would refer to the total nuclear isospin and its z-component, respectively. The  $T$  and  $T_z$  are reserved to distinguish between various two-body interaction channels.

## II. THE BOGOLYUBOV TRANSFORMATION AND SELF-CONSISTENT SYMMETRIES

The starting point of our considerations are the eigenstates of a *deformed* phenomenological single-particle potential. The basis states can be divided into two groups with respect to the signature symmetry ( $\hat{R}_x = e^{-i\pi\hat{j}_x}$ ) quantum number  $r = -i(+i)$  which are later labeled as  $\alpha(\tilde{\alpha})$ , respectively. Two different types of nucleonic pairs can therefore be formed, namely  $\alpha\tilde{\beta}$  and  $\alpha\beta$  pairs. A generalized BCS (gBCS) theory has to account for a scattering of these two types of nucleonic pairs simultaneously. In fact, this work is restricted to pairing in the same and signature reversed states i.e. for  $\alpha\tilde{\alpha}$  and  $\alpha\alpha$  modes only, see also [11].

The signature symmetry cannot be used as a self-consistent symmetry (SCS) in gBCS calculations. Indeed, in such a case the pairing tensor,  $\kappa = \mathbf{V}^*\mathbf{U}^T$ , connects only states of opposite signature [32]. Consequently, the  $\alpha\alpha$   $np$ -pairing cannot be activated, see also [18,19]. Therefore, to take into account simultaneously  $\alpha\tilde{\alpha}$  and  $\alpha\alpha$  pairing one needs to extend the Bogolyubov transformation. The most general Bogolyubov transformation can be written as:

$$\hat{a}_k^\dagger = \sum_{\alpha>0} (U_{\alpha k} a_\alpha^\dagger + V_{\tilde{\alpha} k} a_{\tilde{\alpha}} + U_{\tilde{\alpha} k} a_{\tilde{\alpha}}^\dagger + V_{\alpha k} a_\alpha) \quad (1)$$

where  $\alpha(\tilde{\alpha})$  denote *single particle* states (including isospin indices) of signature  $r = -i(+i)$  respectively, while  $k$  denotes quasiparticles. As discussed above, by superimposing any SCS one always excludes certain interaction channels in the mean-field approximation. Nevertheless, the use of SCS appear many times inherent to the nature of the physical problem and of course, make the theory more transparent and easier to handle numerically. Therefore, prior to construct a general theory involving the transformation (1) we simplify the problem by superimposing (beyond parity) the so called *antilinear simplex symmetry*,  $\hat{S}_x^T = \hat{P}\hat{T}\hat{R}_z$ , as SCS, see [32,18]. One should bear in mind that due to the antilinearity of  $\hat{S}_x^T$  the transformation properties of creation and destruction operators with respect to  $\hat{S}_x^T$  will depend on the phases of the basis states, i.e. no new quantum number can be related directly to this symmetry.

When superimposing  $\hat{S}_x^T$  as the SCS it is rather convenient to choose the phase convention in such a way that the basis states will have exactly the same transformation properties with respect to both  $\hat{R}_x$  and  $\hat{S}_x^T$  and:

$$\hat{S}_x^T \begin{pmatrix} a_\alpha^\dagger \\ a_{\tilde{\alpha}}^\dagger \end{pmatrix} (\hat{S}_x^T)^{-1} = i \begin{pmatrix} -a_\alpha^\dagger \\ a_{\tilde{\alpha}}^\dagger \end{pmatrix} \quad (2)$$

Let us divide our quasiparticle states (1) into two families denoted as  $k$  and  $\tilde{k}$ , respectively:

$$\begin{aligned} \hat{a}_k^\dagger &= \sum_{\alpha>0} (U_{\alpha k} a_\alpha^\dagger + V_{\tilde{\alpha} k} a_{\tilde{\alpha}} + U_{\tilde{\alpha} k} a_{\tilde{\alpha}}^\dagger + V_{\alpha k} a_\alpha) \\ \hat{a}_{\tilde{k}}^\dagger &= \sum_{\alpha>0} (U_{\tilde{\alpha}\tilde{k}} \hat{a}_{\tilde{\alpha}}^\dagger + V_{\alpha\tilde{k}} \hat{a}_\alpha + U_{\alpha\tilde{k}} \hat{a}_\alpha^\dagger + V_{\tilde{\alpha}\tilde{k}} \hat{a}_{\tilde{\alpha}}). \end{aligned} \quad (3)$$

Enforcing  $\hat{S}_x^T$  symmetry as SCS requires that the quasiparticle operators of eq. (3) have the same transformation properties with respect to  $\hat{S}_x^T$  as the single particle operators (2) [32]. This leads to the following restrictions for the coefficients of the Bogolyubov transformation (3):

$$\left\{ \begin{array}{l} U_{\alpha k} = U_{\alpha k}^* \\ U_{\tilde{\alpha}\tilde{k}} = U_{\tilde{\alpha}\tilde{k}}^* \\ V_{\tilde{\alpha} k} = V_{\tilde{\alpha} k}^* \\ V_{\alpha\tilde{k}} = V_{\alpha\tilde{k}}^* \\ \mathbf{Real} \end{array} \right\} \quad \left\{ \begin{array}{l} U_{\tilde{\alpha} k} = -U_{\tilde{\alpha} k}^* \\ U_{\alpha\tilde{k}} = -U_{\alpha\tilde{k}}^* \\ V_{\tilde{\alpha}\tilde{k}} = -V_{\tilde{\alpha}\tilde{k}}^* \\ V_{\alpha k} = -V_{\alpha k}^* \\ \mathbf{Imaginary} \end{array} \right\}. \quad (4)$$

The formalism is complex but the density matrix,  $\rho = \mathbf{V}^*\mathbf{V}^T$ , and pairing tensor  $\kappa = \mathbf{V}^*\mathbf{U}^T$  take the relatively simple structure with real and imaginary blocks decoupled from each other:

$$\rho = \begin{pmatrix} \mathbf{Re}(\rho_{\alpha\beta}) & 0 \\ 0 & \mathbf{Re}(\rho_{\tilde{\alpha}\tilde{\beta}}) \end{pmatrix} + i \begin{pmatrix} 0 & \mathbf{Im}(\rho_{\alpha\tilde{\beta}}) \\ \mathbf{Im}(\rho_{\tilde{\alpha}\beta}) & 0 \end{pmatrix} \quad (5)$$

$$\kappa = \begin{pmatrix} 0 & \mathbf{Re}(\kappa_{\alpha\tilde{\beta}}) \\ \mathbf{Re}(\kappa_{\tilde{\alpha}\beta}) & 0 \end{pmatrix} + i \begin{pmatrix} \mathbf{Im}(\kappa_{\alpha\beta}) & 0 \\ 0 & \mathbf{Im}(\kappa_{\tilde{\alpha}\tilde{\beta}}) \end{pmatrix} \quad (6)$$

Furthermore, the complex structure of the single particle potential  $\mathbf{\Gamma}$  and the pairing potential  $\mathbf{\Delta}$

$$\Gamma_{\alpha\beta} \equiv \sum_{\gamma\delta} \bar{v}_{\alpha\gamma\beta\delta} \rho_{\delta\gamma} \quad \text{and} \quad \Delta_{\alpha\beta} \equiv \frac{1}{2} \sum_{\gamma\delta} \bar{v}_{\alpha\beta\gamma\delta} \kappa_{\gamma\delta} \quad (7)$$

and consequently the gBCS equations are fully determined by the  $\rho$  and  $\kappa$  matrices, respectively.

In this work we define the two-body  $np$ -pairing interaction in terms of an extension of the standard seniority pairing interaction. It is separable in the particle-particle channel,  $\bar{v}_{\alpha\beta\gamma\delta} \propto g_{\alpha\beta} g_{\gamma\delta}^*$ , with  $g_{\alpha\beta}$  proportional (up to a phase factor) to the overlap  $\langle \alpha_\tau | \beta_{\tau'} \rangle$  between the single-particle wave functions.<sup>2</sup> As already mentioned it takes essentially  $\alpha\bar{\alpha}$  and  $\alpha\alpha$  types of pairing, see Sect. III for further detail. To further visualize the physical implications of the  $\hat{S}_x^T$  let us consider the limits of isospin ( $N = Z$  case without Coulomb force) and time reversal symmetry (non-rotating case). Let us consider  $\alpha\bar{\alpha}$  pairing which in principle consists of both T=1 and T=0 components of the  $np$ -pairing. By decomposing the pairing potential into the different isospin components T, T<sub>z</sub> one finds:

$$\Delta_{\alpha t_z, \alpha - t_z}^{(1,0)} \propto \kappa_{\alpha 1/2, \alpha - 1/2} + \kappa_{\alpha - 1/2, \alpha 1/2} \quad \text{and} \quad \Delta_{\alpha t_z, \alpha - t_z}^{(0,0)} \propto \kappa_{\alpha 1/2, \alpha - 1/2} - \kappa_{\alpha - 1/2, \alpha 1/2} \quad (8)$$

i.e. the T=1 and T=0 components of  $np$ -pairing depend on the combinations of the same elements of the pairing tensor but with opposite sign. This is due to the phase relation for the Clebsh-Gordan coefficients which is (anti-)symmetric with respect to the interchange of a proton and neutron for T=(0)1, respectively. Time reversal symmetry further implies that [11]:

$$\kappa_{\alpha 1/2, \alpha - 1/2} = -\kappa_{\alpha 1/2, \alpha - 1/2}^* = \kappa_{\alpha - 1/2, \alpha 1/2}^* \quad (9)$$

and therefore

$$\Delta_{\alpha t_z, \alpha - t_z}^{(1,0)} \propto \text{Re}(\kappa_{\alpha 1/2, \alpha - 1/2}) \quad \text{and} \quad \Delta_{\alpha t_z, \alpha - t_z}^{(0,0)} \propto \text{Im}(\kappa_{\alpha 1/2, \alpha - 1/2}) \quad (10)$$

Consequently, with the pairing tensor of the form of (6), the T=0 component of  $\alpha\bar{\alpha}$  is ruled out through the  $\hat{S}_x^T$  symmetry. Similar analysis shows that T=1 component of the  $\alpha\alpha$  pairing also vanishes due to symmetry reasons.

The latter is well justified due to the Pauli principle. The lack of T=0  $\alpha\bar{\alpha}$  is a deficiency of our model. However, for  $\hbar\omega = 0$  the  $\alpha\bar{\alpha}$  and  $\alpha\alpha$   $np$ -pairing phases are in many applications indistinguishable due to time-reversal symmetry. Since our interaction is essentially structureless, based on pair counting we expect our results not to be sensitive to this restriction. For  $\hbar\omega \neq 0$ , on the other hand, one wants to associate the T=0,  $\alpha\alpha$  ( $\alpha\bar{\alpha}$ )  $np$ -pairing with the coupling to maximum (minimum) spin, respectively. The retained component is expected to be dominant but only at high spins. In order to probe the transition from low to high spin regime one has to explore all possible T=0 pairs and allow for an unconstrained interplay between the different pairing modes. Note, however, that again due to the simplicity of our interaction certain features of the transitional regime can be simulated to some extent with an isospin broken hamiltonian. Indeed, the missing T=0  $\alpha\bar{\alpha}$  component is expected to respond to nuclear rotation in a similar way as T=1  $\alpha\bar{\alpha}$ . It was shown explicitly in Ref. [33] for a single  $j$ -shell model.

In conclusion, in our model the  $\alpha\bar{\alpha}$  pairing is equivalent to T=1 and  $\alpha\alpha$  to T=0 and the isospin notation will be used in the following. This simple analysis reveals also the *important* role the *self-consistent symmetries* can play in theoretical description of  $np$ -pairing in the mean-field theory, see also [10].

### III. THE MODEL HAMILTONIAN

The multipole-multipole expansion offers a rather good approximation to the pairing energy when neutrons and protons can be treated separably. In the following we extend this idea to the case of  $np$ -pairing by constructing a generalized pairing force separable in the particle-particle channel:

$$\hat{V}_{pair} = \frac{1}{4} G \sum_{\alpha\beta} \bar{v}_{\alpha\beta\gamma\delta} \hat{a}_\alpha^\dagger \hat{a}_\beta^\dagger \hat{a}_\delta \hat{a}_\gamma \equiv -\frac{1}{4} \sum_{\alpha\beta} g_{\alpha\beta} \hat{a}_\alpha^\dagger \hat{a}_\beta^\dagger \circ \sum_{\gamma\delta} g_{\gamma\delta}^* \hat{a}_\delta \hat{a}_\gamma \quad (11)$$

where  $g_{\alpha\beta} \equiv \langle \alpha | \hat{G} | \beta \rangle$  and  $\hat{G}$  is an auxiliary operator generating the specific pairing mode with strength  $G$ . The antisymmetry of the two-body matrix element  $\bar{v}_{\alpha\beta\gamma\delta}$  implies that

<sup>2</sup>Subscript  $\tau$  in  $\alpha_\tau$  is necessary to distinguish between proton or neutron single-particle states.

$$\langle \alpha | \hat{G} | \beta \rangle = -\langle \beta | \hat{G} | \alpha \rangle \quad \forall \quad \alpha, \beta. \quad (12)$$

and therefore, the generators  $\hat{G}$  must be *antilinear* and *antihermitian*. We assume here that the correlation energy of the nucleonic pair is proportional to the overlap  $\langle \alpha_\tau | \beta_{-\tau} \rangle$  between single-particle states they occupy (extended seniority-type pairing interaction). The  $\hat{G}$  can then be chosen, for example, as:

$$\hat{G}_{\tau\tau} = \hat{T}, \quad \hat{G}_{np}^{\alpha\bar{\alpha}} = \hat{G}_{np}^{T=1} = \frac{1}{\sqrt{2}} \hat{\tau}_x \hat{T}, \quad \hat{G}_{np}^{\alpha\alpha} = \hat{G}_{np}^{T=0} = \frac{1}{\sqrt{2}} \hat{\tau}_y \hat{S}_x^T \quad (13)$$

for  $pp(nn)$  pairing,  $\alpha\bar{\alpha}$  type of  $np$ -pairing and  $\alpha\alpha$  of  $np$ -pairing. This choice is, however, not unique. In particular, it depends on the choice of the relative phases between neutron and proton states. The choice of phase convention induces strict transformation rules for the isospin Pauli operators  $\hat{\tau}_i$ ,  $i = x, y, z$  with respect to time reversal symmetry [34]. Constructing the generators (13) we assumed the same phases for proton and neutron states ( $|\alpha_\tau, r, \tau\rangle$  denotes the basis state  $\alpha$  of signature  $r = \pm i$  and isospin  $\tau = 1(-1)$  for neutrons(protons)):

$$\hat{T} |\alpha_\tau, r = \mp i, \tau\rangle = \mp |\alpha_\tau, r = \pm i, \tau\rangle \quad (14)$$

Our phase convention further implies that:

$$\begin{aligned} \hat{T} \hat{\tau}_x |\alpha_\tau, r = \pm i, \tau\rangle &= \hat{T} |\alpha_\tau, r = \pm i, -\tau\rangle = \mp |\alpha_\tau, r = \mp i, -\tau\rangle \\ \hat{\tau}_x \hat{T} |\alpha_\tau, r = \pm i, \tau\rangle &= \mp \hat{\tau}_x |\alpha_\tau, r = \mp i, \tau\rangle = \mp |\alpha_\tau, r = \mp i, -\tau\rangle \end{aligned} \quad (15)$$

leading to  $\hat{T} \hat{\tau}_x \hat{T}^{-1} = \hat{\tau}_x$ . Similar considerations for  $\hat{\tau}_y$  and  $\hat{\tau}_z$  operators give:

$$\begin{aligned} \hat{T} \hat{\tau}_x \hat{T}^{-1} &= +\hat{\tau}_x \\ \hat{T} \hat{\tau}_y \hat{T}^{-1} &= -\hat{\tau}_y \\ \hat{T} \hat{\tau}_z \hat{T}^{-1} &= +\hat{\tau}_z \end{aligned} \quad (16)$$

It is straightforward to prove that, with the above phases, the operators (13) satisfy the antilinearity and antihermicity requirements formulated in Eq. (12).

As a main consequence of the separability of the pairing interaction there exists an average gap parameter:

$$\Delta_{\alpha\beta} = \frac{1}{2} \sum_{\gamma\delta} \bar{v}_{\alpha\beta\gamma\delta} \kappa_{\gamma\delta} = -g_{\alpha\beta} \left\{ \frac{G}{2} \sum_{\gamma\delta} g_{\gamma\delta}^* \kappa_{\gamma\delta} \right\} \equiv -g_{\alpha\beta} \Delta \quad (17)$$

Using the generators (13) we obtain:

$$\Delta_{\alpha\tau\beta\tau}^{T=1} = -\delta_{\alpha\tau\beta\tau} \Delta_{\tau\tau}^{T=1} \quad \text{where} \quad \Delta_{\tau\tau}^{T=1} = G_{\tau\tau}^{T=1} \sum_{\alpha_\tau > 0} \kappa_{\alpha_\tau \tilde{\alpha}_\tau} \quad (18)$$

$$\Delta_{\alpha\tau\beta-\tau}^{T=1} = -\langle \alpha_\tau | \beta_{-\tau} \rangle \Delta_{np}^{T=1} \quad \text{where} \quad \Delta_{np}^{T=1} = \frac{1}{2} G_{np}^{T=1} \sum_{\alpha_n \beta_p > 0} \langle \alpha_n | \beta_p \rangle \left\{ \kappa_{\alpha_n \tilde{\beta}_p} + \kappa_{\beta_p \tilde{\alpha}_n} \right\} \quad (19)$$

$$\begin{aligned} \Delta_{\alpha\tau\beta-\tau}^{T=0} &= i\tau \langle \alpha_\tau | \beta_{-\tau} \rangle \mathbf{Im}(\Delta_{np}^{T=0}) \quad \text{and} \quad \Delta_{\alpha\tau\beta-\tau}^{T=0} = -i\tau \langle \alpha_\tau | \beta_{-\tau} \rangle \mathbf{Im}(\Delta_{np}^{T=0}) \\ \text{where} \quad \Delta_{np}^{T=0} &= \frac{i}{2} G_{np}^{T=0} \sum_{\alpha_n \beta_p > 0} \langle \alpha_n | \beta_p \rangle \left\{ \mathbf{Im}(\kappa_{\alpha_n \tilde{\beta}_p}) - \mathbf{Im}(\kappa_{\beta_p \tilde{\alpha}_n}) \right\} \end{aligned} \quad (20)$$

for  $pp(nn)$  pairing,  $T=1$ ,  $\alpha\bar{\alpha}$  type of  $np$ -pairing and  $T=0$ ,  $\alpha\alpha$  of  $np$ -pairing, respectively.

The single-particle potential  $h$  takes the following form

$$h_{\alpha\beta} = e_\alpha \delta_{\alpha\beta} - \omega j_{\alpha\beta}^{(x)} + \Gamma_{\alpha\beta} \quad (21)$$

where the single-particle energies,  $e_\alpha$ , are calculated using a deformed Woods-Saxon potential [35]. Nuclear rotation is included using the cranking approximation [36] and  $\Gamma$  originates from the contribution of the pairing interaction to the single-particle channel. For  $pp(nn)$  pairing we have:

$$\Gamma_{\alpha\tau\beta\tau}^{T=1} = -G_{\tau\tau}^{T=1} \rho_{\beta\tau\alpha\tau} \quad \Gamma_{\widetilde{\alpha\tau}\widetilde{\beta\tau}}^{T=1} = -G_{\tau\tau}^{T=1} \rho_{\beta\tau\alpha\tau} \quad \Gamma_{\alpha\tau\beta\tau}^{T=1} = iG_{\tau\tau}^{T=1} \mathbf{Im}(\rho_{\beta\tau\alpha\tau}) \quad (22)$$

For T=1,  $\alpha\tilde{\alpha}$   $np$ -pairing we obtain:

$$\left\{ \begin{array}{c} \Gamma_{\alpha\tau\beta\tau'}^{T=1} \\ \Gamma_{\widetilde{\alpha\tau}\widetilde{\beta\tau'}}^{T=1} \\ \Gamma_{\alpha\tau\beta\tau'}^{T=1} \\ \Gamma_{\widetilde{\alpha\tau}\widetilde{\beta\tau'}}^{T=1} \end{array} \right\} = \frac{1}{2} G_{np}^{T=1} \sum_{\gamma_{-\tau}\delta_{-\tau'} > 0} \langle \alpha_{\tau} | \gamma_{-\tau} \rangle \langle \beta_{\tau'} | \delta_{-\tau'} \rangle \left\{ \begin{array}{c} -\rho_{\delta_{-\tau'}\gamma_{-\tau}} \\ -\rho_{\delta_{-\tau'}\gamma_{-\tau}} \\ i\mathbf{Im}(\rho_{\delta_{-\tau'}\gamma_{-\tau}}) \end{array} \right\} \quad (23)$$

Finally, for T=0,  $\alpha\alpha$  mode of  $np$ -pairing we get:

$$\left\{ \begin{array}{c} \Gamma_{\alpha\tau\beta\tau'}^{T=0} \\ \Gamma_{\widetilde{\alpha\tau}\widetilde{\beta\tau'}}^{T=0} \\ \Gamma_{\alpha\tau\beta\tau'}^{T=0} \\ \Gamma_{\widetilde{\alpha\tau}\widetilde{\beta\tau'}}^{T=0} \end{array} \right\} = \frac{1}{2} G_{np}^{T=0} \sum_{\gamma_{-\tau}\delta_{-\tau'} > 0} \langle \alpha_{\tau} | \gamma_{-\tau} \rangle \langle \beta_{\tau'} | \delta_{-\tau'} \rangle \left\{ \begin{array}{c} \rho_{\delta_{-\tau'}\gamma_{-\tau}} \\ \rho_{\delta_{-\tau'}\gamma_{-\tau}} \\ -i\mathbf{Im}(\rho_{\delta_{-\tau'}\gamma_{-\tau}}) \end{array} \right\} \quad (24)$$

#### IV. THE LIPKIN-NOGAMI METHOD

The atomic nucleus is a mesoscopic system and as such never undergoes sharp phase transition. The fluctuations are always of importance in the transition region. The classical example is the mean-field prediction of a sharp superfluid-to-normal phase transition, induced by fast rotation, which is always smeared out in nature. The effect can be accounted for theoretically by restoring particle number and this motivated us to include approximate number-projection in our model.

In our letter [20] we have demonstrated that number projection results in a mixing of the T=0 and T=1 pairing phases already in  $N = Z$  nuclei. This suggests that the exclusiveness of these modes discussed in the literature is due to the mean-field approximation. For example, in the SO(8) model calculations the exact solutions allow for mixing of T=0 and T=1 phases while not the gBCS [37,17]. Recently, it was shown by Goodman [21,22] that the mean-field calculations with a  $G$ -matrix interaction performed in a rich model-space in fact do allow for coexistence of T=0 and T=1 pairing phases. The number-projection technique used in our calculations is known as the Lipkin-Nogami (LN) theory. Below, we will outline the main modifications necessary for applying the LN method to the non-separable proton-neutron system.

The LN theory attempts to construct the state  $|LN\rangle$  where both linear and quadratic constraints ( $\tau\tau' \in \{p, n\}$ ):

$$\langle LN|LN\rangle = 1, \quad \langle LN|\Delta\hat{N}_{\tau}|LN\rangle = 0, \quad \langle LN|\Delta\hat{N}_{\tau}\Delta\hat{N}_{\tau'}|LN\rangle = 0 \quad (25)$$

are simultaneously fulfilled. Variation over the Lipkin-Nogami state  $|LN\rangle$  is equivalent to a restricted HFB-type variation for the *auxiliary* Routhian:

$$\delta\langle LN|\hat{H}^{\omega}|LN\rangle \equiv \delta\langle HFB|\hat{\mathcal{H}}^{\omega}|HFB\rangle \quad (26)$$

where<sup>3</sup>

$$\hat{\mathcal{H}}^{\omega} = \hat{H}^{\omega} - \sum_{\tau} \lambda_{\tau}^{(1)} \Delta\hat{N}_{\tau} - \sum_{\tau\tau'} \lambda_{\tau\tau'}^{(2)} \Delta\hat{N}_{\tau} \Delta\hat{N}_{\tau'} \quad (27)$$

The LN method is not a variational approximation. Only the standard linear constraints for the particle number are taken into account as Lagrange-type variational constraints. The parameters  $\lambda_{\tau\tau'}^{(2)}$  are kept constant during the variational procedure and eventually adjusted self-consistently using three additional subsidiary conditions<sup>4</sup>:

$$\langle \hat{\mathcal{H}}^{\omega} (\Delta\hat{N}_{\tau} \Delta\hat{N}_{\tau'} - \langle \Delta\hat{N}_{\tau} \Delta\hat{N}_{\tau'} \rangle) \rangle = 0. \quad (28)$$

with  $\Delta\hat{N}_{\tau} \equiv \hat{N}_{\tau} - N_{\tau}$ .

<sup>3</sup>Obviously,  $\lambda_{np}^{(2)} = \lambda_{pn}^{(2)}$  and the symmetric form of the auxiliary Routhian (27) is chosen for convenience.

<sup>4</sup>In the following, all averages over  $|HFB\rangle$  state will be denoted as  $\langle \ \rangle$  for simplicity.

At the point of self-consistency  $\hat{\mathcal{H}}_{20}^\omega = 0$ , and the equations (28) can be rewritten as

$$\langle \hat{\mathcal{H}}^\omega |4\rangle \langle 4| \Delta \hat{N}_\tau \Delta \hat{N}_{\tau'} \rangle = 0 \quad (29)$$

where  $|4\rangle \langle 4|$  denotes the projection onto the 4-quasiparticle space. The LN conditions (29) depend therefore only on the two-body residual interaction. These equations form a system of three linear equations:

$$\sum_{\tau''\tau'''} A_{\tau\tau'}^{\tau''\tau'''} x_{\tau''\tau'''} = B_{\tau\tau'} \quad (30)$$

where<sup>5</sup>

$$x_{\tau\tau} = \lambda_{\tau\tau}^{(2)} \quad \text{while} \quad x_{pn} = 2\lambda_{pn}^{(2)} \quad (31)$$

and

$$A_{\tau\tau'}^{\tau''\tau'''} = \langle \Delta \hat{N}_{\tau''} \Delta \hat{N}_{\tau'''} |4\rangle \langle 4| \Delta \hat{N}_\tau \Delta \hat{N}_{\tau'} \rangle \quad (32)$$

$$B_{\tau\tau'} = \langle \hat{V}_{two-body} |4\rangle \langle 4| \Delta \hat{N}_\tau \Delta \hat{N}_{\tau'} \rangle \quad (33)$$

The  $x_{\tau\tau'}$  (or  $\lambda^{(2)}$ ) parameters are therefore equal to:

$$x_{\tau\tau'} = \frac{Det \mathbf{A}^{\tau\tau'}}{Det \mathbf{A}} \quad (34)$$

where  $\mathbf{A}^{\tau\tau'}$  denotes the matrix obtained from matrix  $\mathbf{A}$  by replacing the  $\tau\tau'$ -th column of  $\mathbf{A}$  by the vector  $\mathbf{B}$ .

Obviously, the LN theory is technically an analog of the standard HFB theory but for the routhian (27). The resulting LN equations take therefore the form of HFB equations with the single particle field and pairing field renormalized as follows:

$$h_{\tau\tau'}^{LN} \rightarrow h_{\tau\tau'} + 2\lambda_{\tau\tau'}^{(2)} \rho_{\tau\tau'} \quad \text{and} \quad \Delta_{\tau\tau'}^{LN} \rightarrow \Delta_{\tau\tau'} - 2\lambda_{\tau\tau'}^{(2)} \kappa_{\tau\tau'} \quad (35)$$

The contribution to the total energy/routhian due to the LN corrections can be written as:

$$\delta E_{LN} = - \sum_{\alpha\tau, \beta\tau'} \lambda_{\tau\tau'}^{(2)} \{ \rho_{\alpha\tau, \beta\tau'} (\delta_{\alpha\tau, \beta\tau'} - \rho_{\beta\tau', \alpha\tau}) - \kappa_{\alpha\tau, \beta\tau'} \kappa_{\beta\tau', \alpha\tau}^* \} \quad (36)$$

One should always bear in mind that the LN theory provides a sort of optimal HFB-like wave function being different then the  $|LN\rangle$  state. Therefore the expectation values of all physical operators should be recalculated using the following formula:

$$\langle LN | \hat{Q} | LN \rangle \equiv \langle \hat{Q} \rangle = \langle \hat{Q} \rangle - \sum_{\tau\tau'} \lambda_{\tau\tau'}^{(2)} (\hat{Q}) \langle \Delta \hat{N}_\tau \Delta \hat{N}_{\tau'} \rangle \quad (37)$$

with  $\lambda_{\tau\tau'}^{(2)}(\hat{Q})$  dependent on the operator  $\hat{Q}$  in question. These coefficients can be calculated from the following set of five equations:

$$\langle \hat{Q} \Delta \hat{N}_\tau \rangle = 0, \quad \langle \hat{Q} (\Delta \hat{N}_\tau \Delta \hat{N}_{\tau'} - \langle \Delta \hat{N}_\tau \Delta \hat{N}_{\tau'} \rangle) \rangle = 0. \quad (38)$$

---

<sup>5</sup>The asymmetry is induced by the symmetric form of the routhian (27). Note, however, that the corrections to the  $\Gamma$  and  $\Delta$  potentials due to LN terms comes out to be symmetric, see eq. (35).

## V. NUMERICAL CALCULATIONS

An open question in mean-field calculations with  $np$ -pairing is related to the strength of the interaction. Whereas the strength of the  $pp$ - and  $nn$ -seniority pairing force can be established by a fit to the odd-even mass differences, very little is known about the strength of the  $np$ -pairing force. Based on isospin invariance arguments, it seems well justified to assume that at the  $N \sim Z$  line  $G_{pp(nn)}^{T=1} \sim G_{np}^{T=1}$ . Therefore, we will take in the following  $G_{np}^{T=1} = (G_{nn}^{T=1} + G_{pp}^{T=1})/2$  with  $G_{nn(pp)}^{T=1}$  calculated using the average gap method of Ref. [38]. Concerning the strength of the isoscalar  $np$ -interaction we will present most of our results as a function of the parameter  $x^{T=0}$  that scales the strength of  $T=0$   $np$ -pairing interaction with respect to  $G_{np}^{T=1}$  i.e.  $x^{T=0} = G_{np}^{T=0}/G_{np}^{T=1}$ . In some cases, however, we will show examples of solutions for the hamiltonian with broken isospin symmetry.

The discussion is divided into two parts. In section V A we shall concentrate on the solutions for non-rotating cases. Subsections V A 1 and V A 2 briefly recall major properties of the solutions of both unprojected (lateron called BCS) and number-projected (lateron called BCSLN) versions of the model. In subsection V B, we will discuss a procedure allowing to estimate locally, i.e. in relatively narrow range of mass number  $A$ , a 'physical' value of the scaling parameter  $x_0^{T=0}$ . In subsection V C we shall present the results of cranked, number projected calculations demonstrating different aspects of the interplay between mean-field, pairing forces and nuclear rotation.

### A. The frequency zero case

#### 1. Basic properties of the BCS solutions

Let us first briefly recall the main properties of the BCS model solutions without number-projection [20,17]. Let us start with the solutions for self-conjugated  $N = Z$  nuclei. Disregarding the Coulomb interaction and assuming that  $G_{pp}^{T=1} = G_{nn}^{T=1} = G_{np}^{T=1}$  leads to  $\Delta_{pp}^{T=1} = \Delta_{nn}^{T=1} = \Delta_0$ . The solutions fall then into three classes depending on the value of  $x^{T=0}$ :

- (i) For  $x^{T=0} < 1$  ( $G_{np}^{T=0} < G_{np}^{T=1}$ ) the  $T=1$  pairing is energetically favored over the  $T=0$  pairing. The pairing energy depends only on  $\Delta^2 \equiv 2\Delta_0^2 + (\Delta_{np}^{T=1})^2$  and *no* energy is gained by activating the  $T=1$   $np$ -pairing. Note that in our model all pairing phases can be simultaneously present in contrast to the results presented in Ref. [39].
- (ii) The solution at  $x^{T=0} = 1$  ( $G_{np}^{T=0} = G_{np}^{T=1}$ ) is highly degenerate. The BCS energy depends only on  $\Delta^2 \equiv 2\Delta_0^2 + (\Delta_{np}^{T=1})^2 + |\Delta_{np}^{T=0}|^2$ . Also in this limit, no energy is gained due to  $np$ -pairing.
- (iii) The solution at  $x^{T=0} > 1$  ( $G_{np}^{T=0} > G_{np}^{T=1}$ ) corresponds to a pure  $T=0$   $np$ -pairing phase.

For  $N \neq Z$  the main features of the BCS solutions can be characterized as follows:

- (iv) The  $T=1, T_z=0$   $np$ -pairing never forms a collective phase.
- (v) There exists a critical value of the  $x^{T=0}$  parameter,  $x_{crit}^{T=0}$ . For  $x^{T=0} < x_{crit}^{T=0}$  only the  $T=1, |T_z|=1$  solution exist while for  $x^{T=0} \geq x_{crit}^{T=0}$  the  $T=1, |T_z|=1$  and  $T=0$  phases are mixed.
- (vi) The value of  $x_{crit}^{T=0}$  sharply increases with increasing neutron/proton excess  $|T_z|$ . In consequence there exists a critical value  $|\mathbf{T}_z^{crit}|$  above which there is no collective solution for  $np$ -pairing. Our calculations show that this value is small ( $|\mathbf{T}_z^{crit}| \sim 2$ ), see next subsection.

Many of the above properties can be understood in terms of the variational approach, inherent to the (generalized) BCS-formalism. For the case of equal weight of each pair, the system will always choose only that kind of pairs that result in the lowest energy of the system, i.e. result in a sharp phase transition from  $T=0$  to  $T=1$  and vice versa. An interesting feature of the gBCS solution is the 'redundant' role of the  $T=1$   $np$ -pairing in our model when applied to even-even nuclei. It does not mix with the other pairing phases and only in  $N = Z$  nucleus it coexists with  $|T_z|=1$  pairing. Similar properties were found in Ref. [17]. In the particular case of an  $N=Z$  nucleus, the coexistence of  $T=1$  pairing phases at  $x^{T=0}=1$  is very fragile. After switching on the Coulomb force the  $T=1$   $np$ -pairing phase essentially vanishes. On the other hand, for odd-odd nuclei, one expects the  $T=1, |T_z|=0$  pairing to play a role.

The gBCS solutions for isosymmetric  $N = Z$  nuclei have been analyzed analytically in Ref. [11] assuming time-reversal invariance and spherical-symmetry in isospace i.e.  $\langle \hat{\mathbf{T}}_i \rangle = 0$  for  $i = x, y, z$ . It has been demonstrated that coherent,  $np$ -paired, solutions can be obtained for this case provided that  $\rho_{\alpha p, \alpha p} = \rho_{\alpha n, \alpha n}$  and  $\kappa_{\alpha p, \alpha \bar{p}} = -\kappa_{\alpha n, \alpha \bar{n}}$ . The



method of Ref. [11] can be generalized to  $N \neq Z$  nucleus by extending symmetry condition to  $\langle \hat{\mathbf{T}}_i \rangle = 0$  for  $i = x, y$  and  $\langle \hat{\mathbf{T}}_z \rangle = (N - Z)/2$ . For  $N \neq Z$  nuclei, however, neither  $|\rho_{\alpha p, \alpha p}| = |\rho_{\alpha n, \alpha n}|$  nor  $|\kappa_{\alpha p, \bar{\alpha} p}| = |\kappa_{\alpha n, \bar{\alpha} n}|$ . It is then rather straightforward to show, using the HFB conditions  $\boldsymbol{\rho} \boldsymbol{\kappa} = \boldsymbol{\kappa} \boldsymbol{\rho}^*$  and  $\boldsymbol{\rho}^2 - \boldsymbol{\rho} = \boldsymbol{\kappa} \boldsymbol{\kappa}^*$ , that the gBCS theory does not allow for  $np$   $T=1$  pairing solutions. For details, see Appendix A. This result relates the strong limitations of possible solutions of the generalized BCS theory to the underlying symmetries. In this particular example the limitations are due to the time-reversal symmetry and the symmetries ('deformations') in isospace.

In our model,  $\langle \hat{\mathbf{T}}_y \rangle = 0$ , due to the particular form of the density matrix (5). We could verify numerically for a number of examples that the BCS solutions for an isospin invariant hamiltonian are realized at  $\langle \hat{\mathbf{T}}_x \rangle = \langle \hat{\mathbf{T}}_y \rangle = 0$  independent on  $x^{T=0}$ . This is not surprising since our interaction is symmetric in isospin space. For an isospin broken hamiltonian with  $G_{np}^{T=1} > G_{pp(nn)}^{T=1}$  and with an overcritical value of  $G_{np}^{T=1}$  the solutions for  $N \neq Z$  nuclei are triaxial in the isospace i.e. with  $\langle \hat{\mathbf{T}}_x \rangle \neq 0$ , see also discussion in Appendix A.

One may further extend the gBCS model and include an isospin cranking term,  $-\mu \hat{T}_x$ . Such a model can be considered as the lowest-order approximate isospin-projected gBCS theory. One-dimensional isospin rotations have been studied in Ref. [40] in an exactly soluble model including  $T=1$  pairing correlations only. It has been demonstrated that the isospin-cranking solutions rather poorly approximate the exact solutions but the particle-number projected isospin-cranking model offers a very good approximation to the exact solution. Note, that the isospin-cranking model may have several interesting analogies to the well-studied cranking approximation for spatial rotations. Due to the transformation rules of the isospin operators under time-reversal (16) which are different than those for ordinary angular momentum operators, there may also exist basic differences. Neither the possible analogies nor the differences were studied so far. The isospin cranking model in its simplest one-dimensional or more sophisticated three-dimensional version, including both  $T=0$  and  $T=1$   $np$ -pairing correlations, may provide important clues on the role of  $np$ -pairing in excited configurations.

## 2. Basic properties of the BCSLN solutions

The BCSLN solution is qualitatively similar to BCS. The major differences can be summarized as follow:

- (i) Both the critical value of  $x_{crit}^{T=0}$  as well as the 'physical' value of  $x_0^{T=0}$ , extracted according to the prescription of subsection VB are larger in the BCSLN model than in BCS. For self-conjugated  $N = Z$  nuclei, however, the ratio of  $x_{crit}^{T=0}/x_0^{T=0}$  is very similar in both BCSLN and BCS models while for  $T_z \neq 0$  this ratio is smaller in number-projected theory.
- (ii) For self-conjugated  $N = Z$  nuclei, the solutions of BCSLN allow for mixing of the  $T=1$ ,  $|T_z|=1$  pairing phase with isoscalar  $np$ -pairing but not for the collective isovector  $np$ -pairing phase.

A shift of the critical value of  $x_{crit}^{T=0}$  towards values that are larger than unity for  $N = Z$  nuclei is due to the asymmetric way the Lipkin-Nogami corrections modify the different pairing channels. Whereas the 'normal' constraints on proton and neutron number affect the normal and abnormal densities for protons and neutrons, respectively, the constraint on  $\Delta NZ$  involves an additional constrain on  $\rho_{np}$  ( $\kappa_{np}$ ). It appears (numerically) that  $\lambda_{pn}^{(2)}$  is negative implying that the Lipkin-Nogami correction due to  $np$ -pairing,  $\delta E_{np}^{LN}$ , is positive, i.e. repulsive. Both quantities have opposite sign as compared to the analogous quantities for the like-particle channel, see Fig. 1. It means, that the effective gap parameters are weakened in the  $np$ - and enhanced in  $nn$ - and  $pp$ - channels resulting in the above mentioned shift, see Eq. (35). It is interesting to note, however, that the onset of  $np$ -pairing suppresses like-particle correlations, increasing both  $\lambda_{p(n)}^{(2)}$  and the (attractive) energy contribution  $\delta E_{p(n)}^{(LN)}$  in such a way that the total LN correction  $\delta E_{tot}^{(LN)}$  increases with increasing strength of the isoscalar  $np$ -interaction. Note also, that the LN corrections and  $\lambda^{(2)}$  parameters are strongly peaked for  $N = Z$  nuclei and decrease rapidly with the value of  $|N - Z|$  (Fig. 1).

The  $\lambda^{(2)}$  parameters can be approximately estimated as:

$$\lambda_{p(n)}^{(2)} \approx \frac{1}{2} \frac{\partial^2 E}{\partial Z^2 (N^2)} \quad \text{and} \quad \lambda_{pn}^{(2)} \approx \frac{1}{2} \frac{\partial^2 E}{\partial Z N} \quad (39)$$

where  $E(N, Z)$  is the nuclear binding energy. Using the standard liquid-drop functional form for  $E(N, Z)$  one can show that the leading order contributions to (39) for  $N \approx Z$  nuclei:

$$\lambda_{p(n)}^{(2)} \approx -\frac{1}{9} \frac{a_S}{A^{4/3}} + \frac{a_I}{A} + 2 \frac{a_W}{A} \delta_{N,Z} \quad (40)$$

$$\lambda_{pn}^{(2)} \approx -\frac{1}{9} \frac{a_S}{A^{4/3}} - \frac{a_I}{A} - 2 \frac{a_W}{A} \delta_{N,Z} \quad (41)$$

arise from the surface energy, symmetry energy and Wigner term, respectively. Obviously, these estimates are valid for complete HFBLN calculations including contributions to the  $\lambda^{(2)}$  parameters coming from the particle-hole channel. Nevertheless, the above estimates clearly show that (i)  $\lambda_{p(n)}^{(2)}$  and  $\lambda_{pn}^{(2)}$  have opposite signs and that (ii) an enhancement in both  $\lambda_{p(n)}^{(2)}$  and  $\lambda_{pn}^{(2)}$  is expected for  $N = Z$  nuclei due to the singularity of the Wigner energy. These features are in nice qualitative agreement with our calculations, see Fig. 1. Whether or not this behavior is realistic; reflects deficiencies of the LN number projection scheme [see discussion in Ref. [41]] or calls for isospin-projection remains to be studied.

### B. Estimate of the isoscalar $np$ -pairing strength

In our Letter [20] we have demonstrated that the  $T=0$   $np$ -pairing field can yield a microscopic explanation of the Wigner energy in even-even nuclei. It naturally accounts for the singularity of nuclear masses in  $N = Z$  nuclei. The primary mechanism leading to the Wigner cusp can be viewed as a generalization of the well-known blocking effect with additional neutrons or protons outside an  $N = Z$  core playing a similar role as the odd particle plays in the standard blocking phenomenon. This is visualized schematically in Fig. 2. It needs to be stressed that the generalized blocking is not a specific property of our schematic model but does apply for a more realistic pairing interactions as well, see discussion in [37,42]. Moreover, while the standard blocking mechanism requires different trial wave functions for odd and even systems, the generalized blocking does not. The same trial wave function is used for  $N = Z$  and  $N \neq Z$  nuclei in the case shown in Fig. 2.

The Wigner cusp can be obtained either by an isospin invariant model with  $G^{T=0} > G^{T=1}$  or isospin broken model with  $G_{np}^{T=1} > G_{nn(pp)}^{T=1}$  as shown in [43]. We do not see, however, any particular reason to invoke an isospin-broken model, particularly in the light of the discussion in Refs. [30,31]. In these works both experimental and theoretical arguments are given that the Wigner energy originates essentially from  $T=0$  correlations. From these studies it is however not clear whether it is due to  $np$ -pairing. In fact, in Ref. [44], the  $np$ -pairing mechanism was excluded. Note, however, that all these studies were performed using the nuclear shell-model. The shell-model Hamiltonian is usually written in the particle-particle representation but it can be rewritten in the particle-hole representation using the Pandya transformation [45]. Therefore, in the shell-model there is no distinct division into the pairing- and single-particle field. This division is inherent to mean-field models only. Indeed, the shell-model definition of pairing in terms of  $L = 0, S = 1, T = 1$  and  $L = 0, S = 1, T = 0$  as derived from the  $G$ -matrix interaction in Ref. [46] and used in Ref. [44] to analyze the Wigner energy, is completely inappropriate from the point of mean-field model calculations, see also discussion in Ref. [31,33].

Ref. [31] shows the technique to extract the strength,  $W(A)$ , of the Wigner energy [ $E_W(A) = W(A)|N - Z|$ ] from experimental data. Using this method and assuming that the Wigner energy is indeed due to the isoscalar  $np$ -pairing correlations allows us to determine a 'physical' value of the scaling parameter  $x_0^{T=0} = G_{np}^{T=0}/G_{np}^{T=1}$  simply by matching experimental and calculated values of  $W(A)$ . Note that this prescription is by no means limited to our schematic pairing interaction. Under the assumption that the Wigner energy is indeed due to isoscalar  $pn$ -pairing the method can be used for any pairing interaction to establish an overall scaling factor between isovector and isoscalar part.

Let us stress again at this point, that the 'physical' value  $x_0^{T=0}$  deduced in this subsection refers only to the frequency zero calculations because of the missing  $T=0$   $\alpha\bar{\alpha}$  component. For a pairing force, that contains both  $\alpha\bar{\alpha}$  and  $\alpha\alpha$  components in the  $T=0$  channel, the same prescription to determine the strength can be used. Note that also for this case the same value of  $G_{np}^{T=0}$  will be obtained. Indeed, due to time reversal invariance, the BCS or BCSLN energy gain caused by the  $T=0$  pairing will depend only on the modulus  $|\bar{\Delta}^{T=0}|$  of the total isoscalar gap,  $\bar{\Delta}^{T=0} \equiv (\Delta_{\alpha\alpha}^{T=0}, \Delta_{\alpha\bar{\alpha}}^{T=0})$ , but not on its direction (see discussion in Section V A).

Fig. 3 illustrates calculations for  $pf$ -shell  $A \approx 48$  nuclei. In the calculations we have taken a constant deformation of  $\beta_2 = 0.25$  and included 30 deformed neutron and proton states. The realistic values of  $x_0^{T=0}$  are estimated to be  $\sim 1.13$  and  $\sim 1.30$  for BCS and BCSLN models, respectively, as shown in the figure. We performed similar BCSLN calculations for  $A \approx 76$  nuclei assuming  $\beta_2 = 0.40$  and taking 40 deformed neutron and proton states. In this case we have taken  $W(A) = 47/A$  MeV [31] as a reference value because experimental masses are not available. The calculations yield  $x_0^{T=0} \sim 1.25$  which would imply that  $G^{T=0}$  has a different mass dependence than  $G^{T=1}$ .

In this context one should mention, that the deduced  $1/A$  dependence of  $W(A)$  is essentially due to the fast increase of  $W(A)$  for very light  $sd$ -shell nuclei. For  $sd$ -shell nuclei, however, we expect the  $T=0$  pairing to have a pronounced  $L = 0, S = 1$  component. This component becomes strongly quenched due to the spin-orbit interaction when entering the  $pf$ -shell. The properties of  $T=0$  pairing may change strongly at the border of the  $pf$  and  $sd$ -shells. The  $1/A$

dependence of  $W(A)$  may therefore even be an artefact. With the present set of data one cannot extract a reliable  $A$  dependence of the Wigner energy based only on  $pf$ -shell and heavier nuclei. No doubt, that data on masses along the  $N = Z$  line are urgently required in order to resolve this important question.

The procedure to determine the strength is very sensitive to even small variations in  $x^{T=0}$  particularly for BCS calculations because we are working in the region of the phase transition. Indeed, changing  $x_{\text{BCS}}^{T=0}$  by  $\sim 2\%$  (in  $A \approx 48$  nuclei) affects the Wigner energy by  $\sim 200$  keV, as demonstrated in Fig. 3. Moreover, although  $x_{\text{BCSLN}}^{T=0} > x_{\text{BCS}}^{T=0}$  in  $N = Z$ ,  $A \approx 48$  nuclei, the ratio  $y \equiv x_0^{T=0}/x_{\text{crit}}^{T=0}$  appears to be very similar in both BCS and BCSLN models. However, for  $\mathbf{T}_z \neq 0$  we get  $y_{\text{BCS}} < y_{\text{BCSLN}}$  as shown in Fig. 4. In consequence  $|\mathbf{T}_z^{\text{crit}}|_{\text{BCSLN}} > |\mathbf{T}_z^{\text{crit}}|_{\text{BCS}}$  as expected. The difference is still rather small and  $|\mathbf{T}_z^{\text{crit}}| \sim 2$  independently on the model. Fig. 5 compares calculated (BCSLN model) mass excess  $\Delta E = E(x^{T=0}) - E(x^{T=0} = 1)$  for Cr and Sr isotopes as a function of  $\mathbf{T}_z$ . No pronounced differences are seen between Cr and Sr isotopes although there is clear tendency for  $\Delta E(\mathbf{T}_z)$  to be more spread in heavier nuclei, see also Fig. 4.

The Wigner energy has an additional repulsive component in odd-odd  $N = Z$  nuclei. In [31] it has been demonstrated that the strength of this component  $d(A)_{T=0} \approx W(A)$  i.e. both components of the Wigner energy have, most likely, the same origin. This term can be understood within our pairing theory provided that the odd-spin,  $T=0$  states in  $N = Z$  odd-odd nuclei are not treated on the same footing like even-even nuclei but are interpreted as two-quasiparticle ( $2qp$ ) configurations involving one broken  $np$ -pair. Indeed, treating even-even and odd-odd nuclei on the same footing within the generalized BCS(LN) approach gives no odd-odd versus even-even mass staggering, see Fig. 6. The blocking of a  $T=0$   $np$  quasiparticle, on the other side, would result in an odd-odd versus even-even mass ( $T=0$ ) staggering in  $N = Z$  nuclei due to the  $T=0$  pairing energy, analogous to the standard odd-even mass staggering caused by  $T = 1$  pairing. Although the  $T=0$  ground state in odd-odd nuclei is of  $2qp$  character, it is still an open problem of how to construct a proper trail wave function appropriate for odd-odd nuclei. It seems that the isospin restoration (see discussion in Ref. [28]) may play a key role here.

### C. The cranking calculations

As mentioned previously, our schematic, separable  $np$ -interaction does not allow for  $T=0$   $\alpha\tilde{\alpha}$   $np$ -pairing. In a condensate, that is dominated by  $T=0$   $\alpha\alpha$  pairs, there is little resistance for these pairs to align their angular momenta. Note that this alignment occurs without invoking any pair-breaking mechanism. The alignment is a smooth function of the frequency, and no backbend occurs, see Figure 3 in our letter [20].

In the low spin regime, this is of course an unphysical behaviour. The presence of  $T=0$   $\alpha\tilde{\alpha}$  pairing will invoke the pair-breaking mechanism [33] (low- $J$   $np$ -pairs dominate at low-spin [11]). However, as long as we do not use any physical measure sensitive to the isospin of the  $np$ -pairs the  $T=0$   $\alpha\tilde{\alpha}$   $np$ -pairing can be mocked up by  $T=1$   $\alpha\tilde{\alpha}$   $np$ -pairing and vice-versa via a simple readjustment of the strength (isospin-broken model). Indeed, both modes will respond to nuclear rotation in similar way, i.e. through the pair breaking mechanism which leads to a suppression of this field at high spins.

In contrast to the  $\alpha\tilde{\alpha}$  pairing the  $\alpha\alpha$  type pairing will become enhanced at high rotational frequencies as Coriolis and centrifugal forces align more and more pairs along the axis of collective rotation. Indeed, as shown in [19,20], the  $T=0$  phase composed of high- $J$   $np$ -pairs survives to much higher angular momentum. This is in accordance to recent shell model Monte-Carlo calculations [25]. At very high spins, our schematic  $T=0$   $\alpha\alpha$  pairing is probably somewhat too strong since there is no restriction in the  $J$ -values of the pairs that participate in the scattering. However, in accordance to early calculations, we expect to pick up the main essence of the high spin behaviour.

Fig. 7 shows an illustrative example phase-diagram of the critical frequency (the frequency corresponding to the onset of  $np$ -pairing of  $\alpha\alpha$ ) versus the strength of this force. The calculations were performed using the BCSLN model for the  $N = Z$  nucleus  $^{48}\text{Cr}$  at constant deformation and for  $\hbar\omega \leq 2$  MeV. Filled circles represent calculations with  $G_{pp} = G_{nn} = G_{np}^{\alpha\tilde{\alpha}}$  while open circles correspond to an isospin symmetry broken Hamiltonian with  $G_{np}^{\alpha\tilde{\alpha}} = 1.3G_{pp(nn)}$ . Two things are worth to be noticed: (i)  $\hbar\omega_{\text{crit}}$  is very sensitive to the strength parameter and (ii) the alignment (in this case the alignment of  $f_{7/2}$  quasiparticles) triggers the onset of  $T=0$   $np$ -pairing setting a natural threshold ( $x_t^{\alpha\alpha}$ ) for the process. Above this threshold i.e. for  $x^{\alpha\alpha} < x_t^{\alpha\alpha}$  the value of  $\hbar\omega_{\text{crit}}$  increases very sharply. Therefore, even the optimistic scenario would involve the onset of  $np$ -pairing (if at all possible) around the crossing frequency i.e. in the region which is anyhow the most difficult to describe theoretically. This is in accordance to single- $j$  shell model calculations [33,48].

## D. Terminating states

In the  $pf$ -shell, the state of the art  $0\hbar\omega$  shell-models are able to describe nuclear structure with excellent accuracy up to the maximum spin states (terminating states) which is built upon the pure  $f_{7/2}$  sub-shell, see e.g. [49]. For example, for the case of  $^{48}\text{Cr}$ , the state of maximum spin of  $I = 16^+\hbar$  can be reached within  $\pi f_{7/2}^4 \otimes \nu f_{7/2}^4$  configuration. Particle-hole excitations to  $p_{3/2}$  and  $f_{5/2}$  sub-shells allow further to built states of spin up to  $I = 20^+\hbar$  within the full  $pf$  space. However, already at these spins the states involving cross-shell particle-hole excitations are expected to compete. Unfortunately, with the present-day shell-model techniques it is not feasible to perform calculations within the model space needed to describe states above spin  $I = 16\hbar$ , which in principle should include the whole  $sd$ -shell,  $pf$ -shell and the  $g_{9/2}$  sub-shell.

In the standard cranked mean-field model calculations the collectivity of the rotational band in  $^{48}\text{Cr}$  is essentially exhausted after the simultaneous alignment of  $f_{7/2}$  neutrons and protons [49] and one enters the non-collective, unpaired regime around  $I_x = 16\hbar$ . Building up higher angular momentum states proceed further in discrete jumps, which are due to crossings between single-particle down-sloping and up-sloping routhians at spherical shape. This reoccupation process will finally lead again to the onset of collectivity.

The presence of  $T=0$  correlations at high angular momenta may strongly alter the behaviour of high spin states discussed above. In our model, above the terminating  $I = 16\hbar$  state we observe smooth increase of  $I_x$  versus  $\hbar\omega$  rather than the step-like process expected in standard scenario, see Fig. 8. This is due to the pair scattering from  $d_{3/2}$  and  $f_{7/2}$  into the aligned  $g_{9/2}$  and  $f_{5/2}$  orbits which is *entirely* due to  $T=0$  pairing. Partial occupation of these orbits triggers the onset of collectivity after the terminating state [13]. New experiments targeted to measure the evolution of the rotational band in  $^{48}\text{Cr}$  beyond  $I = 16\hbar$  may therefore shed light into the nature of the mean-field  $T=0$  pairing correlations at high spins. Particularly, the possibility of the  $T=0$  pairing correlations to affect the electromagnetic transition rates. Indeed, without  $T=0$  correlations, the wave functions of high-spin states will have the dominant component of 2p-2h and/or 4p-4h configuration (due to promotion of a  $\pi f_{7/2}\nu f_{7/2}$  pair or  $\pi f_{7/2}^2\nu f_{7/2}^2$  quartet to higher sub-shells). The E2-decay from such a configuration into the 0p-0h ( $\pi f_{7/2}^4 \otimes \nu f_{7/2}^4$ ) state would then be strongly hindered. In contrast,  $T=0$  pairing will cause mixing of these (multi)particle-(multi)hole configurations (collectivity) enhancing the E2 transition amplitudes.

## E. TRS-calculations at superdeformed shape

Nuclear superdeformation (SD) is an extreme case of the spontaneous breaking of spherical symmetry. In this case our  $T=0$  pairing interaction, scattering uniformly  $np$ -pairs, may even be considered as quite a realistic approximation provided that the strength is properly adjusted. The standard total routhian surface (TRS) as well as Skyrme-Hartree-Fock calculations predict SD bands to appear at relatively low excitation energy in  $N \sim Z$  nuclei of  $A \approx 80-90$ . Predicted deformations are  $\beta_2 \sim 0.55$  for  $^{88}\text{Ru}$  and even as large as  $\beta_2 \sim 0.75$  for  $^{88}\text{Mo}$ , see [50,51]. To illustrate the influence of  $T=0$  interaction on nuclear superdeformation we performed TRS calculations for SD  $^{88}\text{Ru}$ . Three variants of the calculations different in the treatment of pairing have been performed: (i) unpaired single-particle (ii) including isovector  $T=1$  pairing only, (iii) including both  $T=0$  and  $T=1$  pairing with  $x^{T=0} = 0.9$ ,  $x^{T=0} = 1.1$ , and  $x^{T=0} = 1.3$ . The dynamical moments of inertia ( $J^{(2)} \equiv dI_x/d\omega$ ) versus rotational frequency resulting from this set of calculation are shown in Fig. 9.

As expected, the calculations (i) and (ii) differ strongly at low spins but converge at higher frequencies where static  $T=1$  pairing correlations are essentially washed out by the Coriolis force. The pronounced kink at  $\hbar\omega \approx 0.75$  MeV in calculations (ii) is due to the simultaneous alignment of the  $h_{11/2}$  protons and neutrons. Choosing the strongly undercritical strength of  $G^{T=0}$ , corresponding to  $x^{T=0} = 0.9$ , results of course in a pair field dominated by  $T=1$  pairs. However, after the  $h_{11/2}$  alignment and the disappearance of static  $T=1$  pairing correlations, the  $T=0$  correlations start to build up, resulting in a somewhat larger moment of inertia as compared to the unpaired case. Clearly, the onset of  $T=0$  pairing is triggered by the alignment. The  $x^{T=0} = 1.1$  corresponds to a slightly undercritical  $G^{T=0}$  strength at low  $\hbar\omega$ . The low frequency hump in  $J^{(2)}$  at  $\hbar\omega \approx 0.3$  MeV is in this case due to the *rotation-induced* phase transition from predominantly  $T=1$  to  $T=0$  pairing [19,20]. For larger values of  $x^{T=0}$  the hump moves towards lower frequencies in accordance with the phase diagram in Fig. 7 discussed in Subsect. V C, and the  $h_{11/2}$  alignment is smoothed out. Moreover, the high-frequency part of  $J^{(2)}$  increases exceeding the 'rigid body' value <sup>6</sup> by up to

---

<sup>6</sup>We use the notation of 'rigid body' value as the one given by calculations without pairing. Note that this moment of inertia

$\approx 30\%$ . Although the increase depends very much on the strength of the T=0 interaction (and essentially vanishes for  $x^{T=0} \leq 0.8$ ) the observation of systematic deviations from the standard T=1 model predictions can be considered as a rather robust indicator of the importance of the stretched i.e.  $\alpha\alpha$  type T=0 correlations at high spins.

## VI. SUMMARY AND CONCLUSIONS

Our work presents a number-projected, cranked mean-field formalism appropriate for the simultaneous treatment of T=1 and T=0 correlations. The number-projection technique is a generalization of the Lipkin-Nogami method. We use a schematic  $np$ -pairing interaction because our interest is to study general properties of  $np$ -paired solutions rather than to reproduce properties of specific nuclei.

Our work shows that the exclusiveness of different pairing phases is inherent to the BCS method. Already approximate number-projection leads to a mixing of the T=0 and T=1 pairing phases. Common for both approaches, though, is that different pairing phases counteract each other.

It is also demonstrated that neutron or proton excess block  $np$ -pairing. This generalized blocking mechanism causes  $np$ -pairing to vanish rapidly when departing from the  $N = Z$  line. The calculations suggest that already at  $|\mathbf{T}_z| \sim 2$  there is essentially no chance to observe any collective  $np$ -pairing. This mechanism serves as a possible microscopic explanation of the Wigner energy at the level of mean-field theory. The even-even versus odd-odd mass staggering in T=0 states of  $N = Z$  nuclei indicates a  $2qp$  structure (one broken  $np$ -pair) of the T=0 states in odd-odd  $N = Z$  nuclei. This will require blocked calculations which are beyond the scope of our present paper.

Our model predicts that the T=0 correlations do not vanish at high spin, in accordance to previous calculations. In the high-spins regime stretched T=0 pairing is predicted to be dominant. The onset of this pairing phase seems to be triggered by the alignment of high- $j$  quasiparticles and the related quenching of isovector pairing correlations. The presence of T=0 pairing at high spins is predicted to increase the moments of inertia as well as to affect the evolution of rotational bands beyond their standard terminating states. The size of this effect depends critically on the strength of the T=0 force in the  $\alpha\alpha$  channel. Below a certain limit, in our case below  $x_{\alpha,\alpha}^{T=0} \leq 0.8$ , the effect will not be seen.

This research was supported in part by the U.S. Department of Energy under Contract Nos. DE-FG02-96ER40963 (University of Tennessee), DE-FG05-87ER40361 (Joint Institute for Heavy Ion Research), DE-AC05-96OR22464 with Lockheed Martin Energy Research Corp. (Oak Ridge National Laboratory), by the Polish Committee for Scientific Research (KBN) under Contract No. 2 P03B 040 14, and by the Swedish Institute.

---

strongly differs from that of a rigid body, which would be a constant.

**APPENDIX A: THE TIME-REVERSAL INVARIANCE, ISOSPACE DEFORMATIONS AND THE BCS SOLUTIONS.**

The time-reversal invariance implies the following relations for the hermitian density matrix and antisymmetric pairing tensor elements [11]:

$$\left\{ \begin{array}{l} \rho_{\alpha\tau,\alpha\tau} = \rho_{\alpha\tau,\alpha\tau}^* \\ \rho_{\alpha\tau,\alpha\tau'} = \rho_{\alpha\tau,\alpha\tau'}^* \\ \rho_{\alpha\tau,\bar{\alpha}\tau} = 0 \\ \rho_{\alpha\tau,\bar{\alpha}-\tau} = -\rho_{\alpha\tau,\alpha-\tau}^* \end{array} \right\} \quad \left\{ \begin{array}{l} \kappa_{\alpha\tau,\bar{\alpha}\tau} = \kappa_{\alpha\tau,\bar{\alpha}\tau}^* \\ \kappa_{\alpha\tau,\alpha-\tau} = \kappa_{\alpha\tau,\alpha-\tau}^* \\ \kappa_{\alpha\tau,\alpha\tau} = 0 \\ \kappa_{\alpha\tau,\bar{\alpha}\pm\tau} = -\kappa_{\alpha\tau,\alpha\pm\tau}^* \end{array} \right\}. \quad (\text{A1})$$

The standard BCS constraints  $\langle \Delta \hat{N} \rangle = \langle \Delta \hat{Z} \rangle = 0$  automatically imply that  $\langle \hat{\mathbf{T}}_z \rangle = (N - Z)/2$ . Superimposing further symmetry constraint  $\langle \hat{\mathbf{T}}_x \rangle = \langle \hat{\mathbf{T}}_y \rangle = 0$  together with time-reversal symmetry induced relations (A1) implies:

$$\langle \hat{\mathbf{T}}_x \rangle = \sum_{\alpha>0} \mathbf{Re}(\rho_{\alpha p,\alpha n}) = \langle \hat{\mathbf{T}}_y \rangle = \sum_{\alpha>0} \mathbf{Im}(\rho_{\alpha p,\alpha n}) = 0 \quad \Rightarrow \quad \rho_{\alpha\tau,\alpha-\tau} = 0 \quad \forall \quad \alpha. \quad (\text{A2})$$

The HFB solutions further demand that the generalized density matrix:

$$\mathfrak{R} = \begin{pmatrix} \rho & \kappa \\ \kappa^\dagger & \mathbf{1} - \rho^* \end{pmatrix} \quad (\text{A3})$$

obeys the idempotency condition  $\mathfrak{R}^2 = \mathfrak{R}$  or, equivalently, satisfies the following relations:  $\rho\kappa = \kappa\rho^*$  and  $\rho^2 - \rho = \kappa\kappa^*$ . These relations impose six constraints on the density matrix and pairing tensor elements which all must be fulfilled simultaneously. They can be written as:

$$\kappa_{\alpha\tau,\alpha-\tau}\rho_{\alpha\tau,\alpha-\tau} + \kappa_{\alpha\tau,\bar{\alpha}-\tau}\rho_{\alpha\tau,\bar{\alpha}-\tau} = 0 \quad (\text{A4})$$

$$\rho_{\alpha\tau,\alpha-\tau}\mathbf{Re}(\kappa_{\alpha\tau,\bar{\alpha}-\tau}) + i\mathbf{Im}(\kappa_{\alpha\tau,\alpha-\tau}\rho_{\alpha\tau,\bar{\alpha}-\tau}^*) = 0 \quad (\text{A5})$$

$$\kappa_{\alpha\tau,\alpha-\tau}(\rho_{\alpha\tau,\alpha\tau} - \rho_{\alpha-\tau,\alpha-\tau}) = \rho_{\alpha\tau,\bar{\alpha}-\tau}(\kappa_{\alpha\tau,\bar{\alpha}\tau} - \kappa_{\alpha-\tau,\bar{\alpha}-\tau}) \quad (\text{A6})$$

$$\kappa_{\alpha\tau,\bar{\alpha}-\tau}(\rho_{\alpha\tau,\alpha\tau} - \rho_{\alpha-\tau,\alpha-\tau}) = \rho_{\alpha\tau,\alpha-\tau}(\kappa_{\alpha\tau,\bar{\alpha}\tau} - \kappa_{\alpha-\tau,\bar{\alpha}-\tau}) \quad (\text{A7})$$

$$\rho_{\alpha\tau,\alpha\tau}^2 + |\rho_{\alpha\tau,\alpha-\tau}|^2 + |\rho_{\alpha\tau,\bar{\alpha}-\tau}|^2 - \rho_{\alpha\tau,\alpha\tau} = -\kappa_{\alpha\tau,\bar{\alpha}\tau}^2 - |\kappa_{\alpha\tau,\alpha-\tau}|^2 - |\kappa_{\alpha\tau,\bar{\alpha}-\tau}|^2 \quad (\text{A8})$$

$$\rho_{\alpha\tau,\alpha-\tau}(1 - \rho_{\alpha\tau,\alpha\tau} - \rho_{\alpha-\tau,\alpha-\tau}) = \kappa_{\alpha\tau,\bar{\alpha}-\tau}(\kappa_{\alpha\tau,\bar{\alpha}\tau} + \kappa_{\alpha-\tau,\bar{\alpha}-\tau}) \quad (\text{A9})$$

$$\rho_{\alpha\tau,\bar{\alpha}-\tau}(1 - \rho_{\alpha\tau,\alpha\tau} - \rho_{\alpha-\tau,\alpha-\tau}) = -\kappa_{\alpha\tau,\alpha-\tau}(\kappa_{\alpha\tau,\bar{\alpha}\tau} + \kappa_{\alpha-\tau,\bar{\alpha}-\tau}). \quad (\text{A10})$$

For  $N = Z$  nuclei, the coherent  $np$ -paired solution can be obtained when  $\rho_{\alpha p,\alpha p} = \rho_{\alpha n,\alpha n}$  and  $\kappa_{\alpha p,\bar{\alpha}p} = -\kappa_{\alpha n,\bar{\alpha}n}$ . This is the solution found by Goodman and we refer reader to the Ref. [11] for further details. For  $N \neq Z$  nucleus however, neither  $|\rho_{\alpha p,\alpha p}| = |\rho_{\alpha n,\alpha n}|$  nor  $|\kappa_{\alpha p,\bar{\alpha}p}| = |\kappa_{\alpha n,\bar{\alpha}n}|$ . Using the relations (A4)-(A10) it is straightforward to show that the additional symmetry (axiality in isospace) (A2) rules out  $np$ -pairing of  $\alpha\bar{\alpha}$  type. Indeed, Eqs. (A7) and (A9) give instantly  $\kappa_{\alpha\tau,\bar{\alpha}-\tau} = 0$ .

- 
- [1] N. Anantaraman and J.P. Schiffer, Phys. Lett. **37B** (1971) 229.
- [2] J.P. Schiffer, Ann. Phys. **66** (1971) 78.
- [3] A. Goswami, Nucl. Phys. **60** (1964) 228.
- [4] A. Goswami and L.S. Kisslinger, Phys. Rev. **140** (1965) B26.
- [5] H.T. Chen and A. Goswami, Phys. Lett. **B24** (1967) 257.
- [6] A.L. Goodman, G.L. Struble, and A. Goswami, Phys. Lett. **B26** (1968) 260.
- [7] J. Bar-Touv, A. Goswami, A.L. Goodman, and G.L. Struble, Phys. Rev. **178** (1969) 178.
- [8] A.L. Goodman, G.L. Struble, J. Bar-Touv, and A. Goswami, Phys. Rev. **C2** (1970) 380.
- [9] H. Wolter, A. Faessler, and P. Sauer, Phys. Lett. **B31** (1970) 516.
- [10] H. Wolter, A. Faessler, and P. Sauer, Nucl. Phys. **A167** (1971) 108.
- [11] A.L. Goodman, Nucl. Phys. **A186** (1972) 475.
- [12] A.L. Goodman, Adv. Nucl. Phys. **11** (1979) 263.
- [13] J. Terasaki, R. Wyss, and P.-H. Heenen, Phys. Lett. **B437** (1998) 1.
- [14] P. Fröbrich, Z. Phys. **236** (1970) 153.
- [15] P. Fröbrich, Phys. Lett. **37B** (1971) 338.
- [16] J. Schwieger, F. Simkovic, and A. Faessler, Nucl. Phys. **A600** (1996) 179.
- [17] J. Engel, S. Pittel, M. Stoitsov, P. Vogel, and J. Dukelsky, Phys. Rev. **55C** (1997) 1781.
- [18] K. Nichols and R.A. Sorensen, Nucl. Phys. **A309** (1978) 45.
- [19] E.M. Müller, K. Mühlhans, K. Neergård, and U. Mosel, Nucl. Phys. **A383** (1982) 233.
- [20] W. Satuła and R. Wyss, Phys. Lett. **B393** (1997) 1.
- [21] A.L. Goodman, Phys. Rev. **C58** (1998) R3051.
- [22] A.L. Goodman, Phys. Rev. **C60** (1999) 014311.
- [23] G. de Angelis, C. Fahlander, A. Gadea, E. Farne, W. Gelletly, A. Aprahamian, D. Bazzacco, F. Becker, P.G. Bizzeti, A. Bizzeti-Sona, F. Brandolini, D. de Acuña, M. De Poli, J. Eberth, D. Foltescu, S.M. Lenzi, S. Lunardi, T. Martinez, D.R. Napoli, P. Pavan, C.M. Petrache, C. Rossi Alvarez, D. Rudolph, B. Rubio, W. Satuła, S. Skoda, P. Spolaore, H.G. Thomas, C. Ur, and R. Wyss, Phys. Lett. **B415** (1997) 217.
- [24] D. Rudolph *et al.*, Phys. Rev. Lett. **76** (1996) 376.
- [25] D.J. Dean, S.E. Koonin, K. Langanke, and P.B. Radha, Phys. Lett. **B399** (1997) 1.
- [26] A. Petrovici, K.W. Schmidt, and A. Faessler, Nucl. Phys. **A647** (1999) 197.
- [27] S. Frauendorf and J. Sheikh, Nucl. Phys. **A645** (1999) 509.
- [28] S. Frauendorf and J. Sheikh, Phys. Rev. **C59** (1999) 1400.
- [29] N. Zeldes, in Handbook of Nuclear Properties, Ed. by D. Poenaru and W. Greiner, Clarendon Press, Oxford, 1996, p. 13.
- [30] D.S. Brenner, C. Wesselborg, R.F. Casten, D.D. Warner, and J.-Y. Zhang, Phys. Lett. **B243** (1990) 1.
- [31] W. Satuła, D. Dean, J. Gary, S. Mizutori, and W. Nazarewicz, Phys. Lett. **B407** (1997) 103.
- [32] A.L. Goodman, Nucl. Phys. **A230** (1974) 466.
- [33] R. Wyss, Proceedings of the International Conference on Nuclear Structure, Gatlinburg 1998, AIP conference proceedings 481, (1999) 151.
- [34] J. Dobaczewski, private communication.
- [35] S. Ówiok, J. Dudek, W. Nazarewicz, J. Skalski, and T. Werner, Comp. Phys. Comm. **46** (1987) 379.
- [36] D.R. Inglis, Phys. Rev. **96** (1954) 1059; **103** (1956) 1786.
- [37] J. Engel, K. Langanke, and P. Vogel, Phys. Lett. **B389** (1996) 211.
- [38] P. Möller and R. Nix, Nucl. Phys. **A536** (1992) 20.
- [39] S. Pittel and J. Dobeš, Nucl. Phys. News, Vol.9 No. 3, (1999) 14.
- [40] H.T. Chen, H. Müther, and A. Faessler, Nucl. Phys. **A297** (1978) 445.
- [41] J. Dobaczewski and W. Nazarewicz, Phys. Rev. **C47** (1993) 2418.
- [42] G. Röpke, A. Schnell, P. Schuck, and U. Lombardo, Phys. Rev. **C61**, (2000) 024306.
- [43] O. Civitarese, M. Reboiro, and P. Vogel, Phys. Rev. **C56** (1997) 1840.
- [44] A. Poves and G. Martinez-Pinedo, Phys. Lett. **B430** (1998) 203.
- [45] S.P. Pandya, Phys. Rev. **103** (1956) 956.
- [46] M. Dufour and A.P. Zucker, Phys. Lett. **B430** (1996) 203.
- [47] W. Satuła and R. Wyss, in preparation.
- [48] J. Sheikh and R. Wyss, to be published.
- [49] E. Caurier, J.L. Egidio, G. Martinez-Pinedo, A. Poves, J. Retamosa, L.M. Robledo, and A.P. Zuker, Phys. Rev. Lett. **75** (1995) 2466.
- [50] T. Bäck, B. Cederwall, R. Wyss, D.R. LaFosse, A. Johnson, J. Cederkäll, M. Devlin, J. Elson, F. Lerma, D.G. Sarantites,

- R.M. Clark, I.Y. Lee, A.O. Macchiavelli, and R.W. Macleod, *Eur. Phys. J.* **A6** (1999) 369.
- [51] R. Wyss and W. Satuła, in preparation.



FIG. 1. Value of the **a**) Lipkin-Nogami parameters  $\lambda^{(2)}$  and **b**) contributions to the total energy  $\delta E_{(LN)}$ , calculated for the  $\mathbf{T}_z = 0$  nucleus  $^{48}\text{Cr}$  and  $\mathbf{T}_z = 1$  nucleus  $^{50}\text{Cr}$ . The total correction to the binding energy (filled triangles) and the constituents due to proton/neutron pairing ( $\diamond$ ) and  $np$ -pairing ( $\circ$ ) are shown separately. Note, that the contribution due to  $np$ -pairing is effectively repulsive.

FIG. 2. Schematic representation of the generalized blocking mechanism due to the neutron excess. Shaded area indicates the single-particle levels which do not contribute to  $np$ -pair scattering.

FIG. 3. Experimental ( $\bullet$ ) and calculated strength  $W(A)$  of the Wigner energy for  $pf$ -shell nuclei. The curves marked as ( $\circ$ ) correspond to the BCSLN model calculations with  $x^{T=0} = 1$  and 1.30, respectively. The curves labeled by ( $\Delta$ ) denote the BCS model calculations with  $x^{T=0} = 1, 1.13$  and 1.15, respectively.

FIG. 4. Values of  $x_0^{T=0}/x_{crit}^{T=0}$  versus  $\mathbf{T}_z$ . Open circles present the BCS model results ( $x_0^{T=0} \approx 1.13$ ) while solid circles mark the BCSLN calculations ( $x_0^{T=0} \approx 1.30$ ) in Cr nuclei. The line denoted by ( $\star$ ) represents BCSLN calculations in Sr nuclei ( $x_0^{T=0} \approx 1.25$ ). See text for further details.

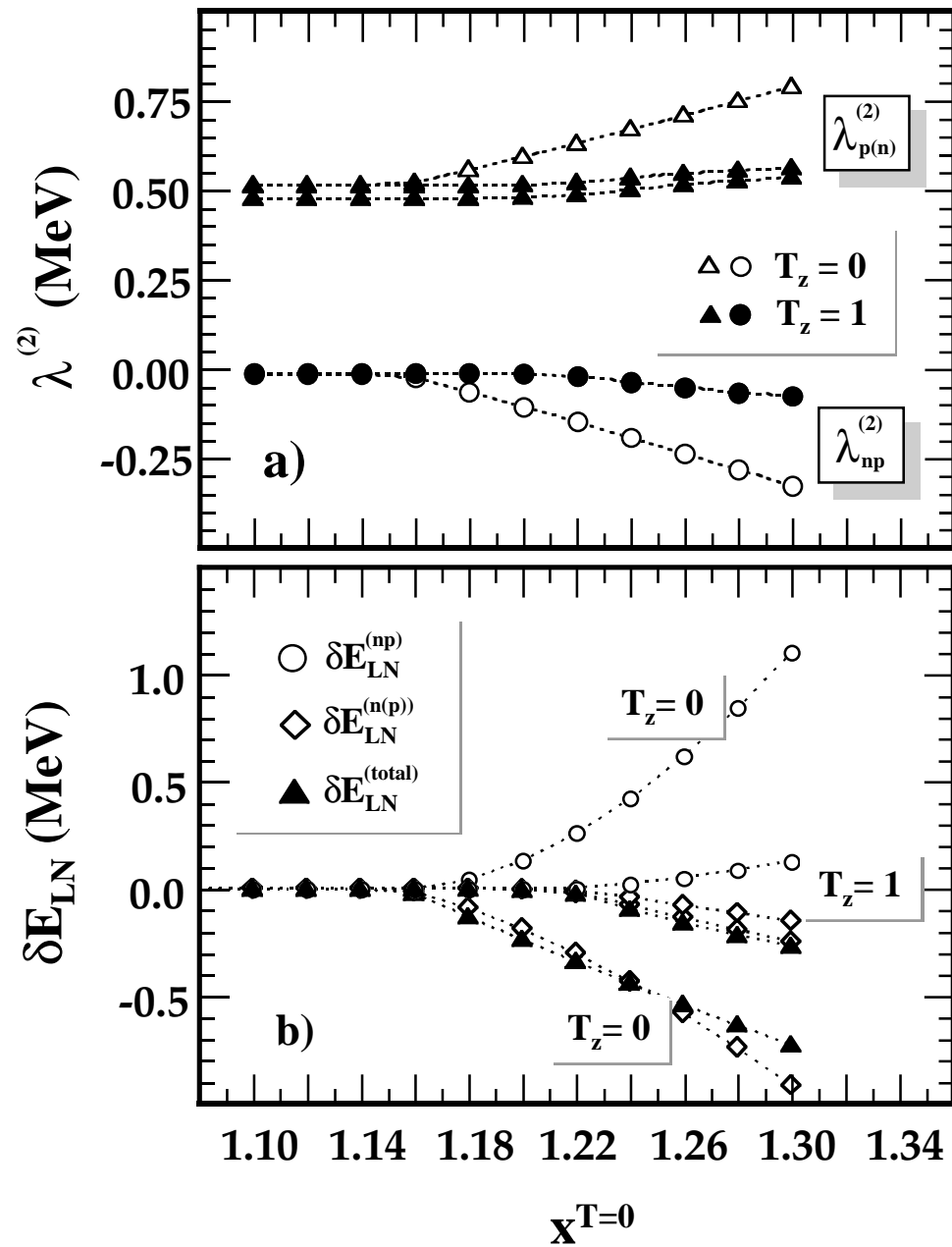
FIG. 5. Calculated mass excess  $\Delta E = E(x^{T=0}) - E(x^{T=0} = 1)$  as a function of  $\mathbf{T}_z$ . The calculations have been performed for Cr (open symbols) and Sr (filled symbols) isotopes and for  $x^{T=0} = 1.1$  ( $\Delta$ ), 1.2 ( $\diamond$ ), 1.3 ( $\circ$ ). The line denoted by ( $\star$ ) corresponds to the 'physical' value of  $x^{T=0} = 1.25$  representative for Sr isotopes. The strength parameters for like-particle correlations were calculated using the average gap method. In our case it yields  $G_{pp} \approx 0.385(0.250)$  MeV for  $Z=24(38)$ , respectively. The difference in the pairing strength,  $\Delta G = G_{nn} - G_{pp}$  versus  $\mathbf{T}_z$  is shown in the insert.

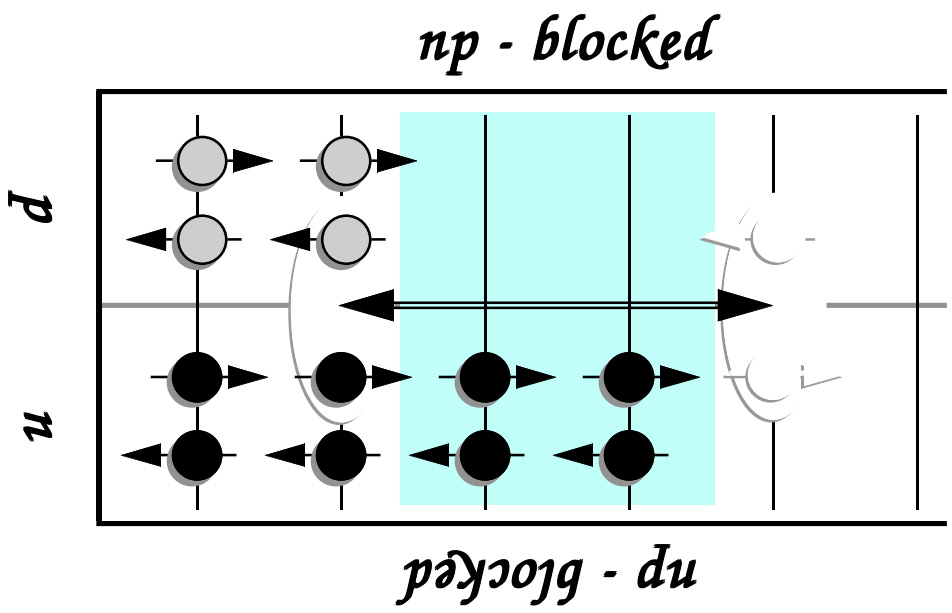
FIG. 6. Experimental ( $\bullet$ ) and calculated ( $\circ, \Delta$ ) correction to the Wigner energy,  $d(A)_{T=0}$ . Note, that both BCS and BCSLN theories give essentially no contribution. For further detail see text.

FIG. 7. Frequency  $\hbar\omega_{crit}$  for the onset of the  $T=0$   $\alpha\alpha$   $np$ -pairing as a function of the strength  $x^{T=0}$  of this force. Calculations were performed for  $^{48}\text{Cr}$  at constant deformation  $\beta_2 = 0.25$  using the BCSLN model. The line marked by ( $\bullet$ ) shows the calculations with an isospin-symmetric hamiltonian i.e. for  $G_{pp}^{T=1} = G_{nn}^{T=1} = G_{np}^{T=1}$  while ( $\circ$ ) denotes the calculations for an isospin-broken hamiltonian with  $G_{np}^{T=1} = 1.3G_{pp(nn)}$ . The vertical arrow marks the position of the crossing frequency of the  $f_{7/2}$  quasiparticles calculated without  $np$ -pairing.

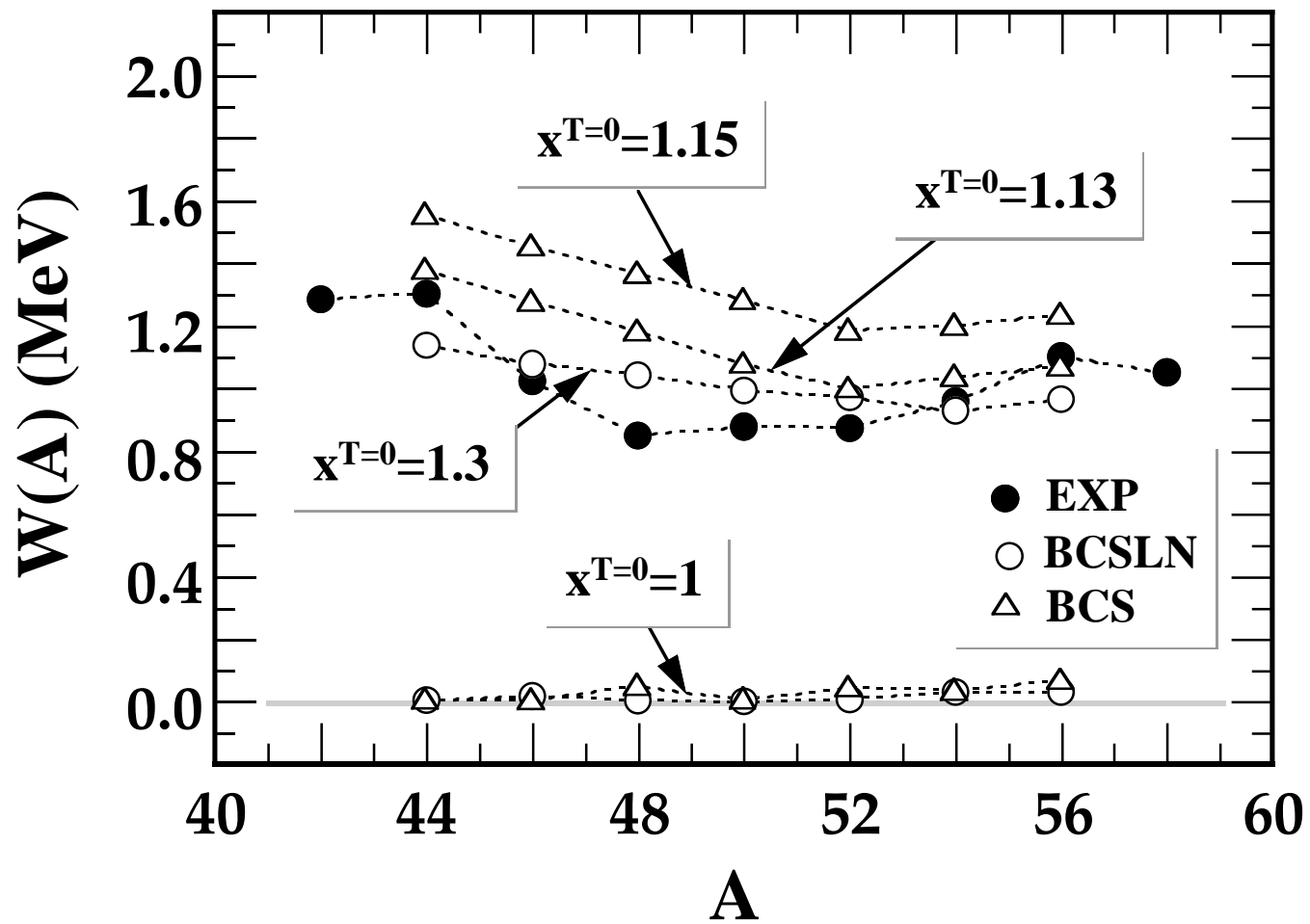
FIG. 8. Gain in angular momentum,  $\delta I_x$ , due to the onset of  $T=0$   $\alpha\alpha$   $np$ -pairing relative to the predictions of a model without  $np$ -pairing. The quantity  $\delta I_x$  was calculated for  $^{48}\text{Cr}$  ( $\beta_2 = 0.25$ ) at high frequency,  $\hbar\omega = 2$  MeV and is shown as a function of the strength parameter  $x^{T=0}$ .

FIG. 9. The dynamical moment of inertia for the SD band in the  $N = Z$  nucleus  $^{88}\text{Ru}$  as a function of  $\hbar\omega$ . Unpaired ( $T=1$  paired) calculations are marked with  $\circ$  ( $\bullet$ ), respectively. The calculations with  $T=0$  pairing are labeled by  $\Delta$  ( $x^{T=0}=0.9$ ),  $\square$  ( $x^{T=0}=1.1$ ), and  $\diamond$  ( $x^{T=0}=1.3$ ). Note the large moments of inertia for the  $T=0$  paired solutions at high frequencies.

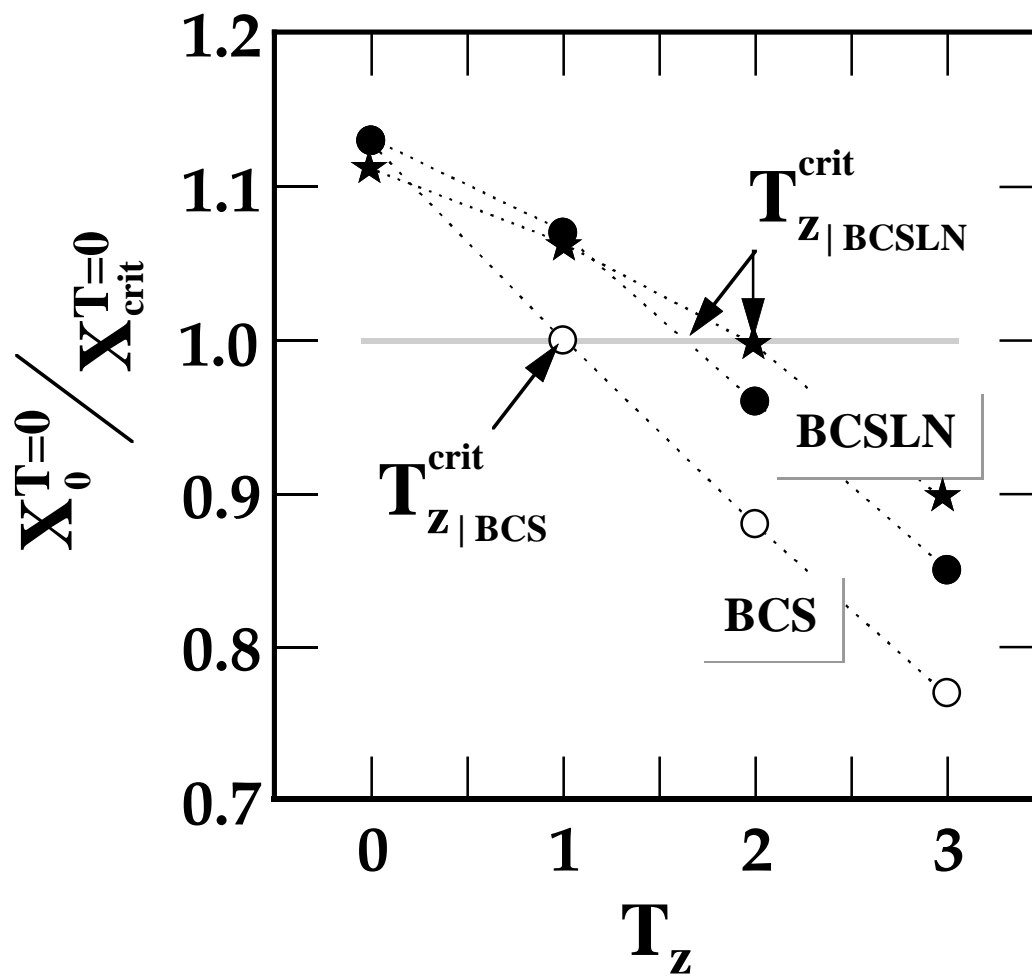




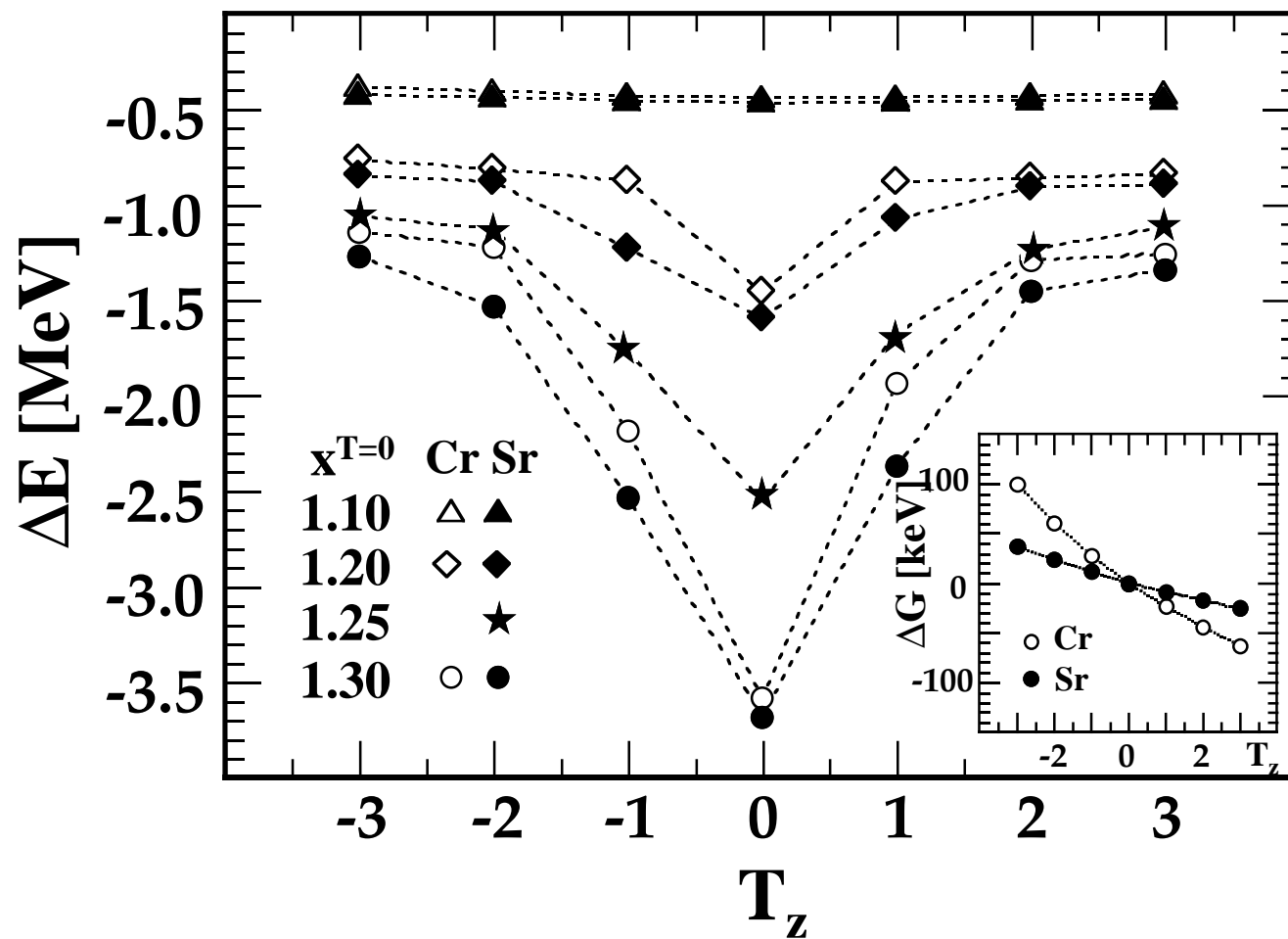
W. Satula & R. Wyss, Figure 2



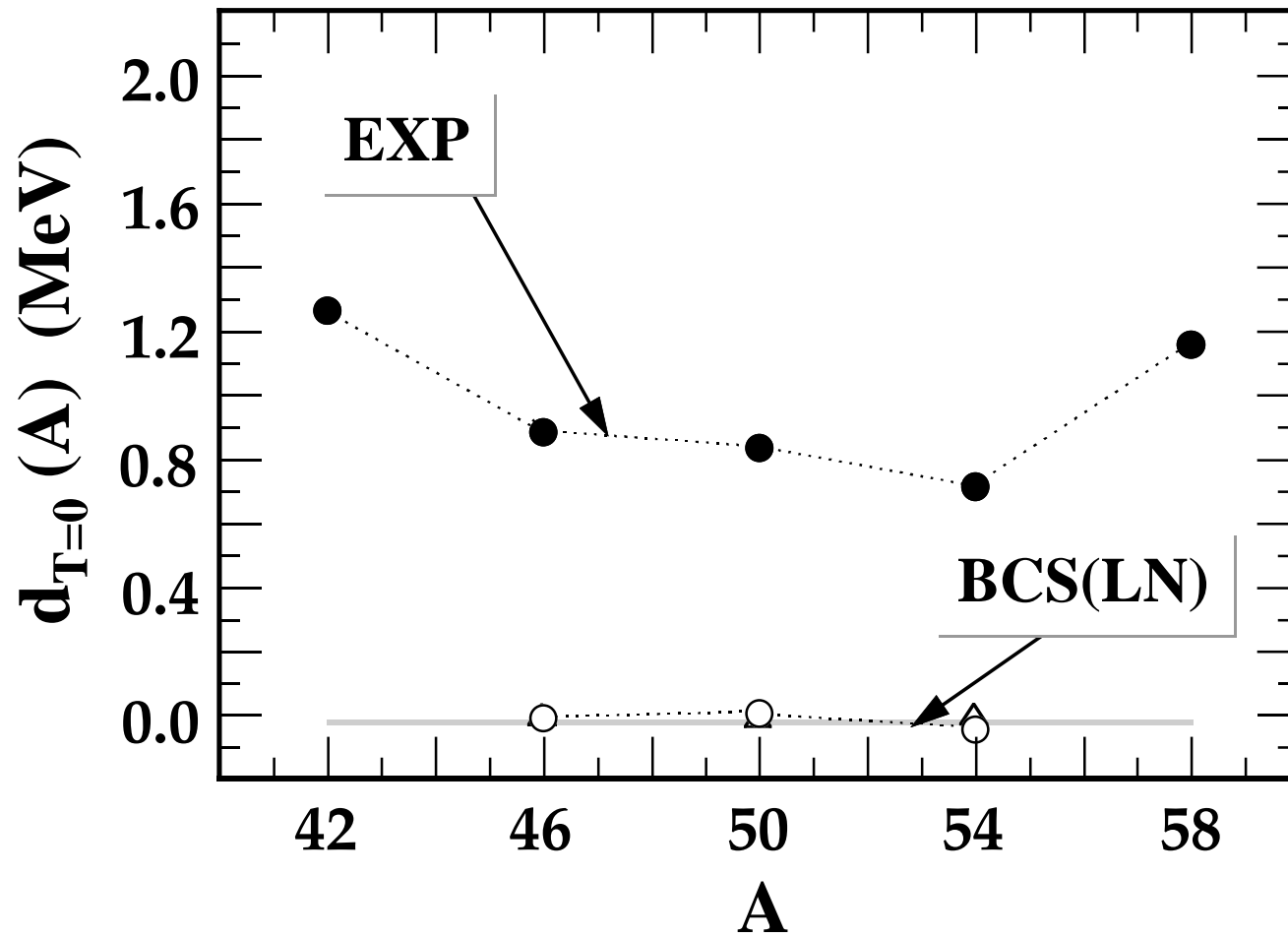
W. Satula & R. Wyss, Figure 3



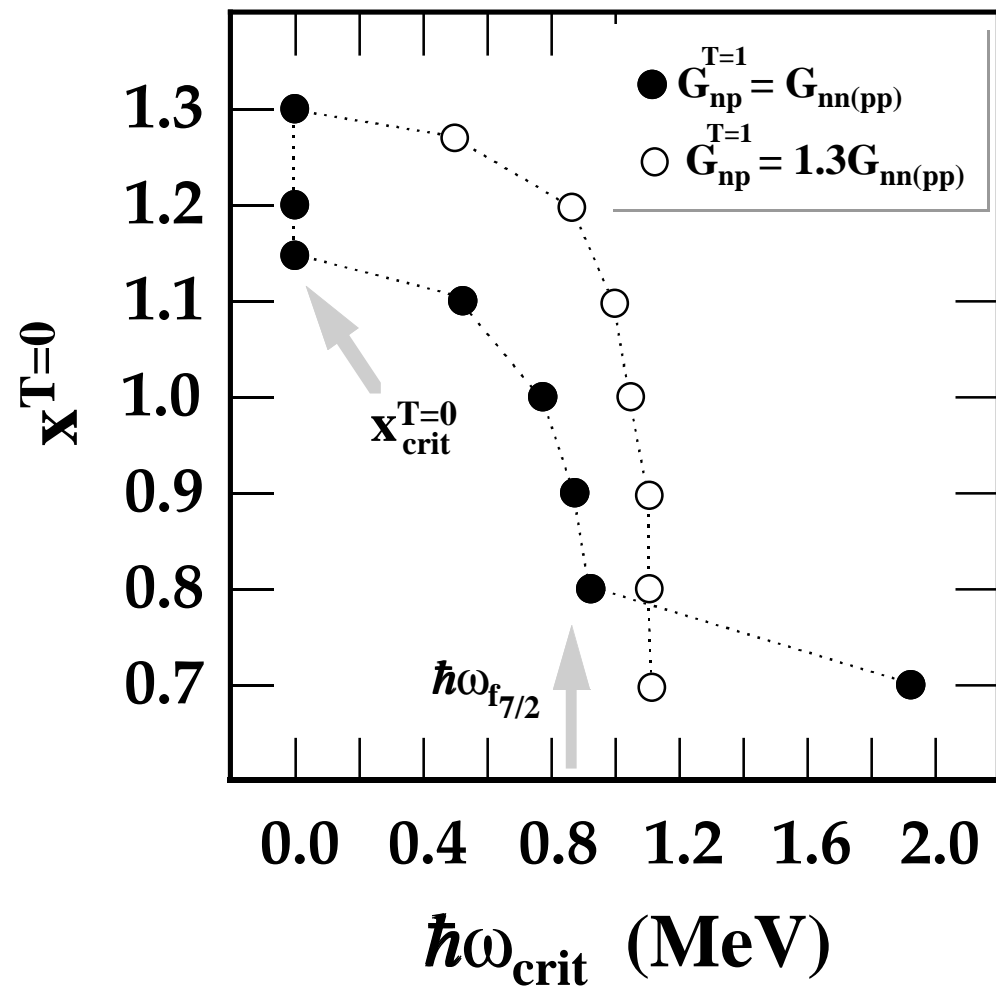
W. Satula & R. Wyss, Figure 4



W. Satula & R. Wyss, Figure 5

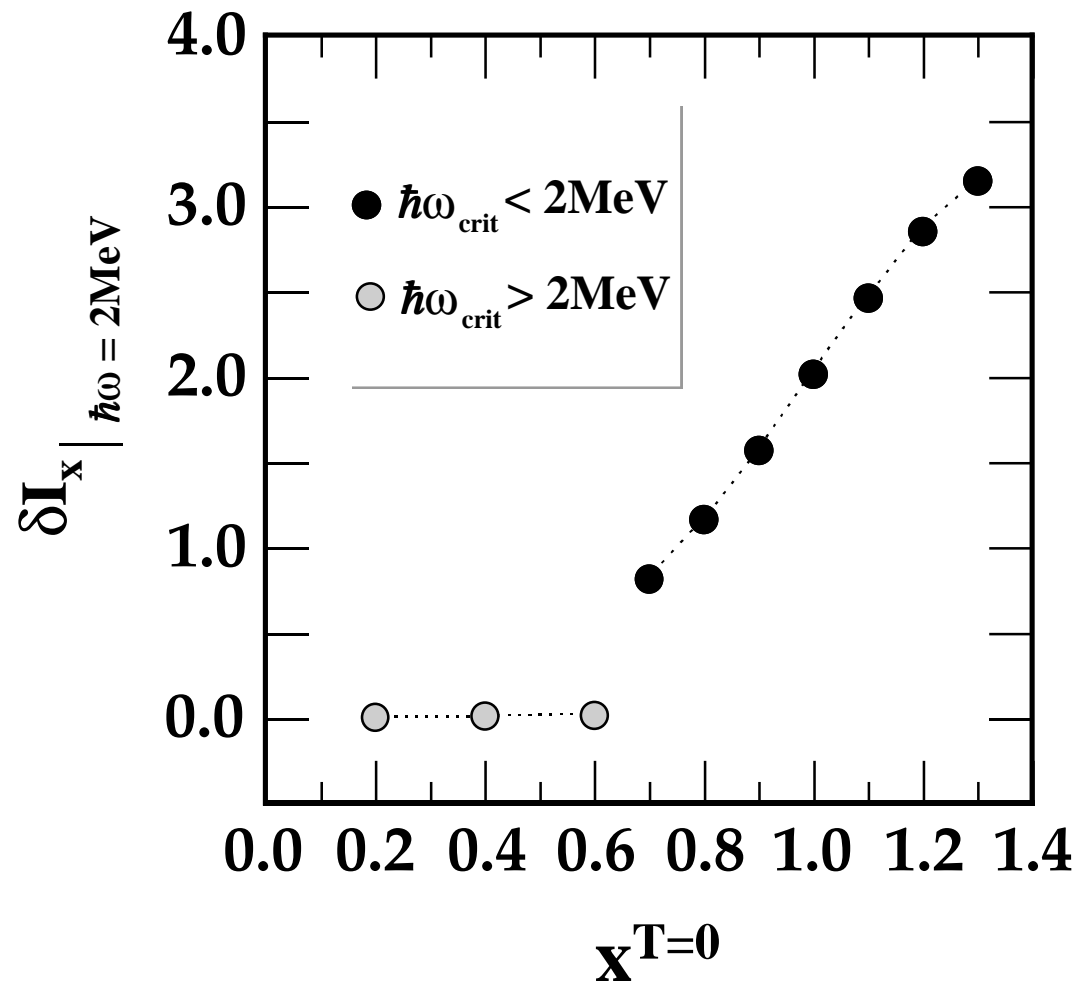


W. Satula & R. Wyss, Figure 6

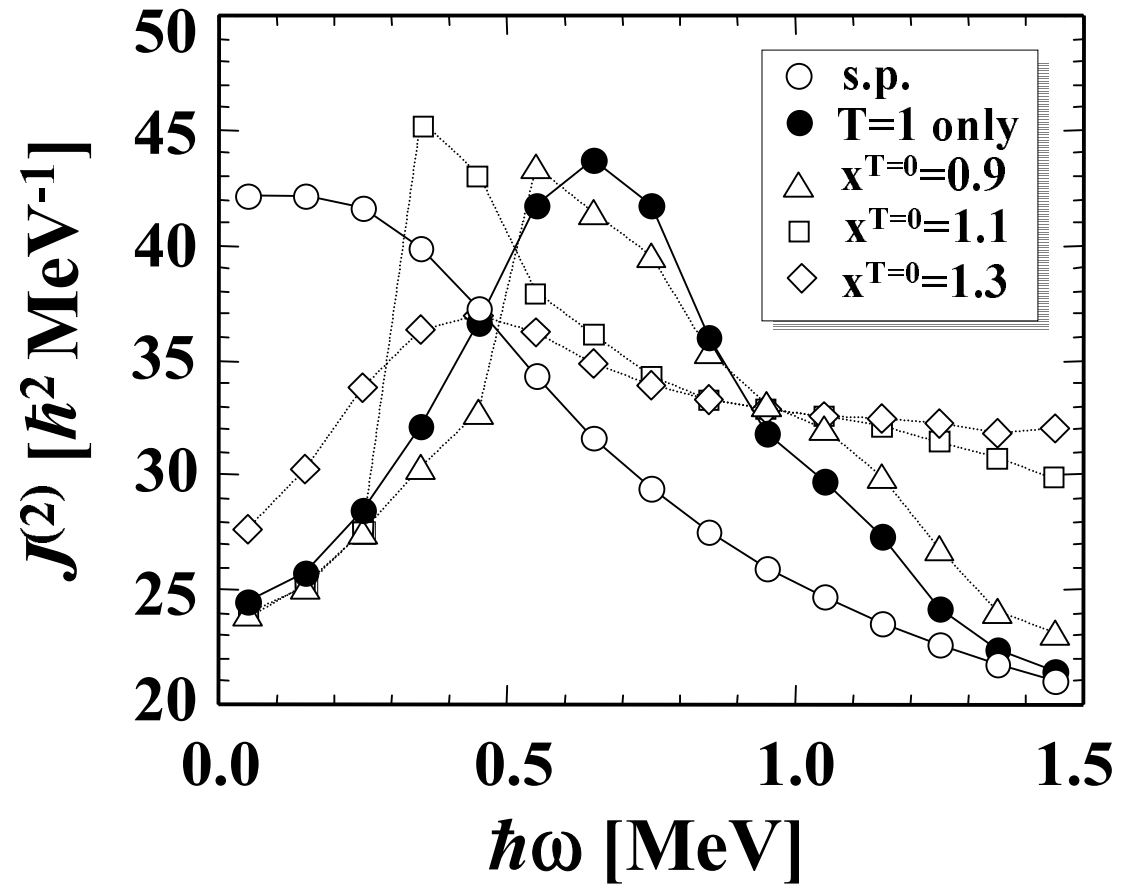


W. Satula & R. Wyss, Figure 7





W. Satula & R. Wyss, Figure 8



W. Satula & R. Wyss, Figure 9